

# **Modeling of Cooling-Water Inleakage Effects in PWR Steam Generators**

---

**NP-1786  
Research Project 404-1**

Topical Report, April 1981

Prepared by

**NWT CORPORATION  
7015 Realm Drive  
San Jose, California 95119**

**Principal Investigators  
J. Leibovitz  
S. G. Sawochka**

Prepared for

**Electric Power Research Institute  
3412 Hillview Avenue  
Palo Alto, California 94304**

**EPRI Project Manager  
C. S. Welty, Jr.**

**Analysis and Testing Program  
Nuclear Power Division**

## **DISCLAIMER**

**This report was prepared as an account of work sponsored by an agency of the United States Government. Neither the United States Government nor any agency thereof, nor any of their employees, makes any warranty, express or implied, or assumes any legal liability or responsibility for the accuracy, completeness, or usefulness of any information, apparatus, product, or process disclosed, or represents that its use would not infringe privately owned rights. Reference herein to any specific commercial product, process, or service by trade name, trademark, manufacturer, or otherwise does not necessarily constitute or imply its endorsement, recommendation, or favoring by the United States Government or any agency thereof. The views and opinions of authors expressed herein do not necessarily state or reflect those of the United States Government or any agency thereof.**

---

## **DISCLAIMER**

**Portions of this document may be illegible in electronic image products. Images are produced from the best available original document.**

## ORDERING INFORMATION

Requests for copies of this report should be directed to Research Reports Center (RRC), Box 50490, Palo Alto, CA 94303, (415) 965-4081. There is no charge for reports requested by EPRI member utilities and affiliates, contributing nonmembers, U.S. utility associations, U.S. government agencies (federal, state, and local), media, and foreign organizations with which EPRI has an information exchange agreement. On request, RRC will send a catalog of EPRI reports.

\_\_\_\_\_

EPRI authorizes the reproduction and distribution of all or any portion of this report and the preparation of any derivative work based on this report, in each case on the condition that any such reproduction, distribution, and preparation shall acknowledge this report and EPRI as the source.

## NOTICE

This report was prepared by the organization(s) named below as an account of work sponsored by the Electric Power Research Institute, Inc. (EPRI). Neither EPRI, members of EPRI, the organization(s) named below, nor any person acting on their behalf: (a) makes any warranty or representation, express or implied, with respect to the accuracy, completeness, or usefulness of the information contained in this report, or that the use of any information, apparatus, method, or process disclosed in this report may not infringe privately owned rights; or (b) assumes any liabilities with respect to the use of, or for damages resulting from the use of, any information, apparatus, method, or process disclosed in this report.

Prepared by  
NWT Corporation  
San Jose, California

## EPRI PERSPECTIVE

### PROJECT DESCRIPTION

RP404 is one of several projects in the Steam Generator Program involving long-term system chemistry monitoring at 17 operating pressurized water reactor (PWR) nuclear power plants. This project focuses on those plants with recirculating steam generators. The corrosion modeling done in RP404 is covered in this topical report.

### PROJECT OBJECTIVE

The widespread occurrence of denting and other forms of corrosion damage in recirculating steam generators is known to be qualitatively related to impurities transported via the feedtrain. A primary source of these impurities is the inleakage of condenser cooling water. By monitoring chemistry performance and long-term trends as related to condenser cooling-water inleakage and relating such trends to observed steam generator corrosion damage, it will be possible to develop design and operating guidelines that can significantly increase the operating life of recirculating steam generators.

### PROJECT RESULTS

In this topical report, the contractor provides the details of an analytic model that may be used to predict the effect of condenser cooling-water inleakage on the corrosion rate of the carbon steel support plates at any given site. Comparison of the analytic model predictions with laboratory corrosion experiments demonstrated that the model can provide insights into observed corrosion damage problems.

This report will be of interest to plant chemistry staffs in predicting the impact of corrodent ingress on steam generator performance, to designers and

architect-engineers in developing condenser and condensate specifications, and in general to PWR owners and operators.

C. S. Welty, Jr., Project Manager  
Steam Generator Project Office  
Nuclear Power Division

## ABSTRACT

Analytical models of solution chemistry in local regions of PWR steam generators with condenser inleakage of seawater, brackish water, cooling tower water and fresh water have been developed. Acidic solutions are expected in crevices at other than fresh water sites; caustic solutions are expected at fresh water sites. While silica input associated with condenser inleakage had a negligible effect on crevice chemistry for the cases considered, silica input to the steam generators from other sources can be sufficiently large to increase crevice acidity at seawater sites during condenser inleakage at steady state blowdown chloride concentrations of 50 to 200 ppb. Modeling results, in conjunction with corrosion estimates as a function of pH, can be employed to develop preliminary estimates of the effect of blowdown water quality on denting at operating plants. Extensive model improvement and verification, complemented by focused laboratory corrosion measurement programs and improved operating plant corrosion assessments, will be necessary to improve the reliability of such estimates.



## CONTENTS

<u>Section</u>	<u>Page</u>
1 INTRODUCTION	1-1
2 SOLUTION CHEMISTRY IN THE ABSENCE OF SILICA	2-1
Model Considerations	2-1
Isolated Cavity Model	2-2
Model	2-2
Results	2-5
Dynamic Equilibrium Model	2-12
Model	2-12
Results	2-12
Implication of Results	2-12
3 SOLUTION CHEMISTRY IN THE PRESENCE OF SILICA	3-1
Model Considerations	3-1
Modeling Results	3-4
4 IMPLICATIONS OF MODELING RESULTS	4-1
5 FUTURE EFFORTS	5-1
REFERENCES	R-1
APPENDIX A DERIVATION OF GOVERNING RELATIONS IN THE ABSENCE OF SILICA	A-1
APPENDIX B DERIVATION OF THE SOLUBILITY PRODUCT FOR SERPENTINE FROM THERMODYNAMIC DATA	B-1
APPENDIX C PHASE DIAGRAM CONSTRUCTION	C-1
APPENDIX D PRECIPITATION CRITERION	D-1



## ILLUSTRATIONS

<u>Figure</u>	<u>Page</u>
2-1 Isolated Cavity pH Variation with Boiling at 280°C	2-9
2-2 Effect of AVT Additives on Isolated Cavity pH at 280°C with Mississippi River Water Ingress	2-10
2-3 Effect of AVT Additives on Isolated Cavity pH at 280°C with Seawater Ingress	2-11
2-4 Effect of AVT Additives on Bulk Coolant pH at 280°C with Alkaline Fresh Water Ingress	2-13
2-5 Effect of AVT Additives on Bulk Coolant pH at 280°C with Seawater Ingress	2-14
3-1 Phase Diagram of Relative Stabilities at 275°C	3-3
3-2 Variation of Isolated Cavity pH with Mississippi River Water Ingress at 280°C	3-5
3-3 Variation of Hydroxyl Ion Concentration in an Isolated Cavity with Mississippi River Water Ingress at 280°C	3-6
3-4 Variation of Isolated Cavity pH with Seawater Ingress at 280°C	3-8
3-5 The Effect of Silica on the Variation of Isolated Cavity pH with Concentration Factor (Temperature at 280°C; Seawater Inleakage to give 50 ppb in Steam Generator)	3-10
4-1 Predicted Crevice pH at a Seawater Plant (Concentration Factor = 10,000)	4-2
4-2 Tube Support Plate Corrosion Rate at Seawater Cooled Plant (Concentration Factor = 10,000)	4-3
4-3 Effect of Blowdown Chloride Concentration on Denting at a Seawater Plant (Concentration Factor = 10,000)	4-5
C-1 Phase Diagram of Relative Stabilities at 275°C	C-4

Blank

X

## TABLES

<u>Table</u>	<u>Page</u>
2-1 Representative Cooling Water Analyses	2-3
2-2 Volatile Chemical Properties	2-4
2-3 Ionic Concentration in Solutions at 280°C	2-6
A-1 Physical Chemistry Relations	A-3
C-1 Solubility Relations	C-2
C-2 Free Energy of Reactions, 275°C	C-3

## SUMMARY

Corrosion of pressurized water reactor (PWR) U-tube steam generators has led to reduced plant availability through increased maintenance and inspection requirements, and in several instances has necessitated total replacement of the Alloy 600 tube bundle. Initially, corrosion attack consisted of Alloy 600 interactions with the sodium phosphate compounds employed for control of steam generator chemistry--in particular, tube cracking, attributed to the presence of free sodium hydroxide, and wastage, attributed to the presence of acidic sodium phosphate derivatives. With recognition of the extreme difficulty of controlling phosphate chemistry within the bounds necessary to achieve long term steam generator tube integrity, recirculating U-tube steam generator vendors specified conversion of chemistry control to all volatile treatment (AVT). The concern with AVT was the impact of condenser inleakage chemicals on boiler water chemistry in the absence of a pH buffering compound, in particular, local formation of caustic solutions and Alloy 600 stress corrosion cracking. However, the major corrosion problem which has been observed is "denting", the inward deformation of the Alloy 600 tubing caused by the corrosion of the carbon steel support plate in the tube to tube support plate crevice. This mode of attack can lead to tube support plate stress levels sufficient to tightly bind the tubes and crack the plate and/or tubes. The severity of denting can be such to necessitate tube bundle replacement.

To understand the reason for the accelerated support plate attack, solution chemistry in local regions was modeled during periods of condenser inleakage of seawater, brackish water, cooling tower water and fresh water, considering the possible precipitation of calcium sulfate, magnesium hydroxide, and calcium hydroxide. Consistent with plant corrosion observations, the model results indicate that concentrated solutions of hydrochloric acid are formed in local regions at seawater and brackish water sited plants during condenser inleakage. Solutions deriving their acidity from sulfuric acid are formed at cooling tower sites employing sulfuric acid for scaling control. At fresh water sites such as those on the Mississippi River and Lake Michigan, basic solutions are formed in local regions, predominantly as a result of the loss of carbon dioxide by volatilization during boiling.

Based on routine chemistry monitoring results from individual utilities, it was recognized subsequently that silica concentrations of 50 to 100 ppb routinely exist in the steam generator blowdown even in the absence of significant cooling water inleakage. The observed silica levels appear indicative of continual low level silica input from makeup water.

To determine analytically the effect of silica on local solution chemistry during condenser inleakage, it was necessary to consider a plethora of possible silicate precipitates, particularly those of calcium and magnesium. This led to identification of six additional precipitates requiring consideration bringing the total to nine. With this number of compounds, development of a computer program yielding convergence over a reasonable time became inadvisable and an alternate approach was sought. A "phase diagram" technique was developed subsequently and allowed identification of the appropriate set(s) of equations to be addressed as evaporation in the crevice proceeded.

Employing this technique, silica was shown to increase crevice acidity during condenser inleakage at seawater and brackish water sites compared to that developed in the absence of silica. At fresh water sites, silica functions as a buffer and reduces the basicity of crevice solutions.

There remain recognized deficiencies in the models that must be addressed to increase the reliability and usefulness of the results. Nonetheless, even in their present form, the models have been of considerable value in developing an understanding of crevice chemistry evolution in local regions. Further model improvements, which are being funded by the Steam Generator Owners Group in EPRI Project S167-1, should allow the modeling results to be employed to develop adequate chemistry guidelines for PWR steam generating systems.

## Section 1

### INTRODUCTION

Pressurized water reactor (PWR) steam generators have experienced extensive corrosion damage, which has resulted in a significant loss in nuclear plant availability. In addition, the requirements for inspection and repair of damage can lead to significant personnel radiation exposure. In an attempt to alleviate the corrosion problems, it has been recommended that leakage of impurities from condensers be reduced to very low levels.

To assess the possible effects of coolant inleakage on steam generator corrosion, it is necessary to consider the variation in chemistry of solutions formed from steam generator bulk water as the steam quality is increased along the length of the generator, as well as of the residual solutions formed in cavities, e.g., in crevices and in porous deposits from which liquid evaporates. Such situations can be approximated by relatively simple models, sufficient to establish chemistry trends at reasonable confidence levels.

Two models have been developed. The first, denoted as the "Dynamic Equilibrium Model", describes the dynamic vapor to liquid equilibrium which exists in the steam generator bulk fluid as the coolant is progressively boiled to higher qualities. This model attempts to predict chemistry variations in a solution initially in the liquid state as steam quality is increased from zero to near 100% at constant mass and constant temperature.

In the second model, denoted as the "Isolated Cavity Model", vapor is allowed to escape as the liquid mass is reduced. Chemical species in each differential amount of escaping vapor are assumed to be in equilibrium with those remaining in the liquid. In both models, liquid phase ionic residues are assumed to be in equilibrium with any solid precipitates.

There are only minor variations between the two models in the computational procedures. Basic to both models are the equilibrium equations relating dissolved species in the liquid residue to each other and to any precipitates which are formed.

Where only one substance can precipitate from an aqueous solution, two possible situations must be considered, i.e., one of sufficiently low concentration without a precipitate, and the other of sufficiently high concentration in equilibrium with the precipitate. Where an additional substance can precipitate, the number of possible situations is doubled, i.e., the number of possible situations increases exponentially with the number  $n$  of possible precipitates, and is expressed by  $2^n$ . In each case, the situation is described by a different set of equations which must be solved simultaneously. As such, the general treatment soon becomes inordinately cumbersome as the number of possible precipitates increases, and an alternate approach is advisable.

In the case of interest, specifically the ingress of condenser cooling water to an operating steam generator, consideration of three possible precipitates generally is accepted as adequate to describe solution chemistry during boiling. In the initial modeling efforts, these three precipitates ( $Mg(OH)_2$ ,  $CaSO_4$ , and  $Ca(OH)_2$ ) were considered by specifically addressing  $2^3$  or 8 sets of equations. A detailed description of and the results derived from the models are presented below.

It subsequently was realized that the anion present at the highest concentration in the bulk steam generator coolant in the absence of condenser inleakage and during periods of low level condenser inleakage was silicate probably as a makeup water impurity. This realization forced consideration of possible silicate precipitates of calcium and/or magnesium and resulted in the development of a novel method based on a phase diagram for solution of the array of 512 sets of equations. This procedure, and the solution chemistry estimates derived therefrom, is also discussed below.

## Section 2

### SOLUTION CHEMISTRY IN THE ABSENCE OF SILICA

#### MODEL CONSIDERATIONS

The species considered in the modeling process are: water solvent,  $H^+$  and  $OH^-$ ,  $NH_3$ ,  $NH_4^+$ ,  $SO_4^{=}$ ,  $HSO_4^-$ ,  $CO_2$ ,  $CO_3^{=}$ ,  $HCO_3^-$ ,  $Cl^-$ ,  $Na^+$ ,  $Ca^{++}$  and  $Mg^{++}$ . The possible precipitates are  $CaSO_4$ ,  $Ca(OH)_2$  and  $Mg(OH)_2$ .

It is necessary to distinguish eight possible situations:

1. No precipitate
2. Only  $CaSO_4$  precipitates.
3. Only  $Ca(OH)_2$  precipitates.
4. Only  $Mg(OH)_2$  precipitates.
5.  $CaSO_4$  and  $Ca(OH)_2$  precipitate but not  $Mg(OH)_2$ .
6.  $CaSO_4$  and  $Mg(OH)_2$  precipitate but not  $Ca(OH)_2$ .
7.  $Ca(OH)_2$  and  $Mg(OH)_2$  precipitate but not  $CaSO_4$ .
8.  $CaSO_4$ ,  $Ca(OH)_2$  and  $Mg(OH)_2$  precipitate.

For each situation, a different set of relations applies and is solved simultaneously by iteration.

Various iterative procedures can be applied with different degrees of success in convergence. A modified Newton-Raphson procedure was found to yield reasonable convergence for all initial solution compositions and for all residual solutions resulting from the concentrating processes encountered to date. (There is no assurance that the same success will be obtained with other solution compositions.)

The derivation of the required eight sets of equations, corresponding to the eight precipitation modes, is presented in Appendix A.

The criteria used to determine which set of equations applies to a given residual solution (before pH is known) are incorporated within the iteration loops. The criteria are established in Appendix A under the "Determination of the Relevant

"Set of Equations" section. The iteration scheme also is discussed in the same section.

Treatment of the volatile species, which is dependent on the specific model (dynamic equilibrium or isolated cavity), is considered in the "Volatiles" section of Appendix A.

The modeling efforts were hampered somewhat by the sparsity of physical chemistry data on ionization products, solubility products, activity coefficients and gas volatilities at high temperature. The major physical chemistry parameters employed during the study are shown in Table A-1 of Appendix A. These properties are felt to represent the most accurate estimates of each parameter available at this time.

For the purpose of this study, cooling water analyses at five operating plants were employed (Table 2-1). For each water type the disposition of major species identified in the cooling water is predicted analytically using both the isolated cavity and dynamic equilibrium models. To set the concentrations in the bulk steam generator coolant, a condenser leak rate of 5 liters/h with a blowdown of 13620 liters/h (60 gpm) is assumed. At such conditions, no precipitate is formed in the bulk coolant. Volatile chemical concentration was set to give a room temperature pH of 9.0. Emphasis was placed on the variation of pH with boiling. In the absence of silica, the major species for which it was necessary to consider precipitation were calcium sulfate, calcium hydroxide, and magnesium hydroxide. Volatilization of carbon dioxide and ammonia also were considered. In the latter stages of the study, variations in solution chemistry with different pH control additives such as morpholine and cyclohexylamine also are examined. Constants for the volatile additives are given in Table 2-2.

#### ISOLATED CAVITY MODEL

##### Model

In the isolated cavity model, a mass of steam generator bulk water is boiled to dryness in a cavity. Additional liquid is not allowed to enter the cavity to dilute the concentrated solution which results from boiling. Steam vapor is allowed to exit the cavity as it is generated. As the solution is boiled away, volatile species enter the steam phase and are removed from the liquid in the cavity. Salts such as calcium sulfate, calcium hydroxide, and magnesium hydroxide precipitate. In the results presented herein redissolution of previously

Table 2-1  
REPRESENTATIVE COOLING WATER ANALYSES

	Mississippi River	Lake Michigan	Brackish	Cooling Tower	Seawater
Calcium, ppm	58	32	44	160	400
Magnesium, ppm	15	11	78	55	1272
Sodium, ppm	13	3.2	603	16	10561
Potassium, ppm	--	--	20	--	380
Chloride, ppm	4.8	2.1	1053	10.5	18980
Carbonate, ppm	0	0	0	0	0
Bicarbonate, ppm	217	149	68	61	142
Total Alk., ppm $\text{CaCO}_3$	178	122	56	50	116
Sulfate, ppm	45	7	220	571	2649
Silica, ppm	14	5	8.6	25	0.01-7.0

Table 2-2  
VOLATILE CHEMICAL PROPERTIES

	<u>Ammonia</u>	<u>Cyclohexylamine</u>	<u>Morpholine</u>
At 25°C			
Concentration, ppm	0.25	1	5
pH	9	9	9
Ionization Constant	$1.77(10^{-5})$	$4.39(10^{-4})$	$2.13(10^{-6})$
At 280°C			
$K_D$ (ppm in steam ppm in solution)	3.7 <sup>a</sup>	12.5 <sup>b</sup>	0.5 <sup>c</sup>
Ionization Constant	$6.76(10^{-7})^d$	$3.0(10^{-6})^e$	$6(10^{-7})^e$

a) Reference (3)

b) Reference (4)

c) Reference (5), assumed independent of temperature and concentration

d) Reference (2)

e) Reference (6), corrected for ionic strength

precipitated salts is allowed, i.e., total equilibrium of all species within the liquid phase including solid precipitates is assumed. The model would be readily modifiable to eliminate redissolution of species precipitated early in the evaporation process. However, this effect is not expected to lead to any significant changes in the results at high concentration factors. The concentration factor is defined as the ratio of the initial to remaining water mass, i.e., the concentration factor would be 10 if a 10 gram sample were evaporated to the point where one gram of water remained in the cavity.

### Results

Concentration of major species for each of the water classes are given in Table 2-3 as a function of concentration factor. These results were obtained using ammonia as a pH control additive. The five cooling waters fall into two general classes: acid or caustic forming. Seawater, brackish water, and cooling tower water form concentrated acid solutions on boiling in an isolated cavity. Both fresh water types form sodium hydroxide solutions upon boiling. Hydrochloric acid is formed with seawater and brackish water. Sulfuric acid is formed with the cooling tower waters treated for carbonate control. Variations in pH with boiling are shown in Figure 2-1 for Mississippi River and seawater cooled waters. As can be seen, pH is depressed approximately two full units at a concentration factor of  $10^3$  for the seawater case and increased greater than two full units for the Mississippi River water case.

Using the model, it is possible also to evaluate the difference in isolated cavity solution chemistry with variation in pH control additive. Differences in the pH with ammonia, cyclohexylamine, and morpholine additives are shown in Figures 2-2 and 2-3 for the Mississippi River water and seawater cases, respectively. These cases bound the variation expected with other cooling water types. In the fresh water cooled case morpholine, which is less volatile than ammonia or cyclohexylamine, initially produces a pH about 0.2 units higher than the other additives. This difference becomes insignificant when the local concentration factor is greater than 20. The model predicted similar effects among the various amines in the seawater cooled plant but with less initial pH difference (Figure 2-3). As magnesium began to precipitate in the seawater case, pH variation was almost identical in solutions of different amines.

Table 2-3  
IONIC CONCENTRATIONS IN SOLUTIONS AT 280°C\*  
ppm

			Local Concentration Factor in Steam Generator				
	1	2	5	10	100	1,000	10,000
<u>Mississippi River</u>							
Bicarbonate	0.08	~0	~0	~0	~0	~0	~0
Bisulfate	0.004	0.008	0.013	0.016	0.027	0.0007	0.0003
Calcium	0.02	0.043	0.11	0.21	2.1	14.6	17.9
Chloride	0.0018	0.0036	0.009	0.018	0.18	1.8	18
pH	5.90	5.92	6.14	6.37	7.13	8.01	8.35
Magnesium	0.0055	0.011	0.028	0.055	0.0106	0.00015	~0
Sodium	0.005	0.01	0.02	0.05	0.5	4.8	48
Sulfate	0.013	0.025	0.07	0.15	1.62	0.4	0.5
<u>Lake Michigan</u>							
Bicarbonate	0.055	~0	~0	~0	~0	~0	~0
Bisulfate	0.0007	0.0014	0.0027	0.0033	0.0063	0.0013	0.0002
Calcium	0.012	0.024	0.06	0.12	1.2	10.9	30.6
Chloride	0.0008	0.0015	0.004	0.008	0.08	0.8	7.8
pH	5.87	5.82	5.99	6.23	6.97	7.85	8.24
Magnesium	0.004	0.008	0.02	0.04	0.023	0.0003	~0
Sodium	0.0012	0.0024	0.006	0.012	0.12	1.2	12
Sulfate	0.002	0.0038	0.01	0.022	0.25	0.5	0.27

Table 2-3 (continued)

	Local Concentration Factor in Steam Generator						
	<u>1</u>	<u>2</u>	<u>5</u>	<u>10</u>	<u>100</u>	<u>1,000</u>	<u>10,000</u>
<u>Brackish</u>							
Bicarbonate	0.03	~0	~0	~0	~0	~0	~0
Bisulfate	0.002	0.047	0.099	0.14	1.2	13.9	214
Calcium	0.016	0.032	0.081	0.16	1.1	0.78	2
Chloride	0.4	0.8	1.9	3.9	39	390	3870
pH	5.85	5.78	5.87	6.04	5.92	5.30	4.37
Magnesium	0.03	0.06	0.14	0.29	2.3	21.8	208
Sodium	0.23	0.45	1.1	2.3	22.6	226	2260
Sulfate	0.06	0.12	0.3	0.67	5.6	30	214
<u>Cooling Tower</u>							
Bicarbonate	0.02	~0	~0	~0	~0	~0	~0
Bisulfate	0.054	0.11	0.23	0.32	1.3	22.4	342
Calcium	0.06	0.12	0.3	0.6	0.6	0.16	0.1
Chloride	0.004	0.008	0.02	0.04	0.4	3.9	39
pH	5.87	5.82	5.95	6.11	6.05	5.53	4.88
Magnesium	0.02	0.04	0.1	0.2	1.5	12.9	114
Sodium	0.006	0.012	0.03	0.06	0.6	5.9	59
Sulfate	0.16	0.31	0.83	1.8	7	46	353

Table 2-3 (continued)

	Local Concentration Factor in Steam Generator						
	<u>1</u>	<u>2</u>	<u>5</u>	<u>10</u>	<u>100</u>	<u>1,000</u>	<u>10,000</u>
<u>Seawater</u>							
Bicarbonate	0.05	0	0	0	0	0	0
Bisulfate	0.19	0.31	0.84	1.9	23	370	5860
Calcium	0.15	0.3	0.7	1.1	1	4.7	108
Chloride	7	14	35	70	700	6960	69600
pH	5.965	6.03	5.93	5.77	5.09	4.03	2.48
Magnesium	0.47	0.94	2.2	4.3	42	400	3700
Sodium	4	8	19.8	39.6	400	3960	39600
Sulfate	0.78	1.6	4.0	6.9	41	263	630

\*Blowdown 13620 l/h (60 gpm)

Leak Rate 5 l/h (0.022 gpm)

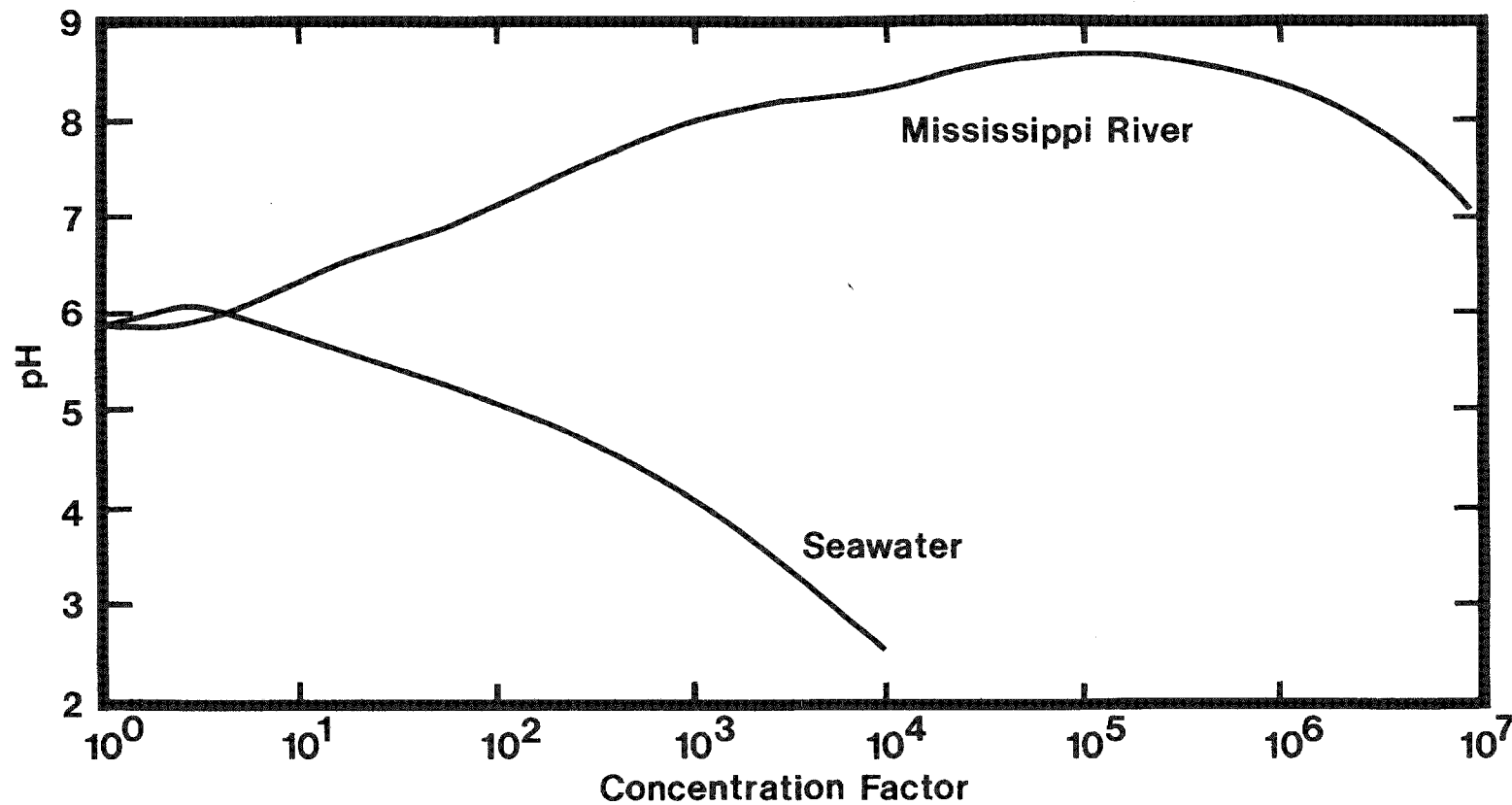


Figure 2-1. Isolated Cavity pH Variation with Boiling at 280°C

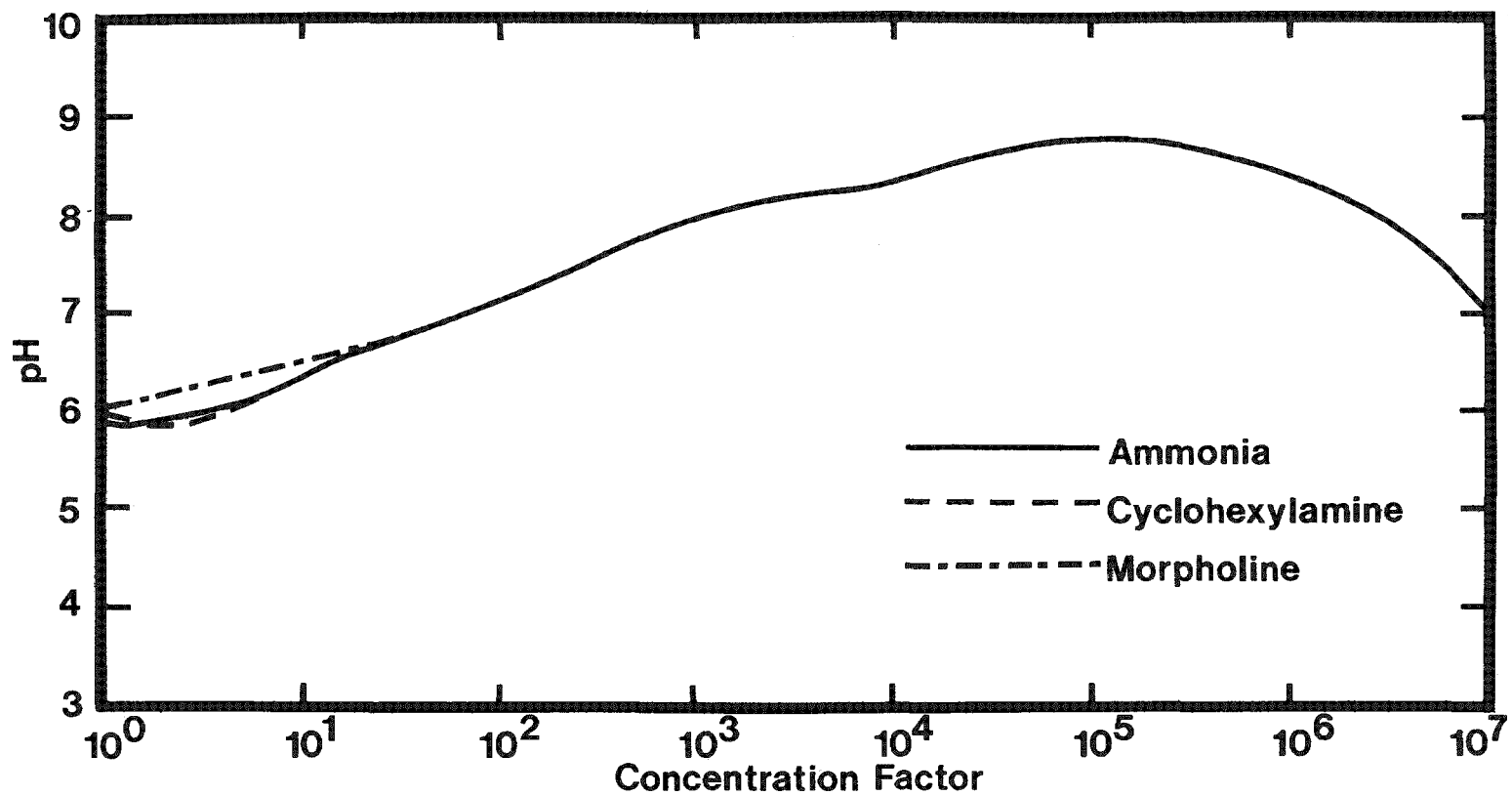


Figure 2-2. Effect of AVT Additives on Isolated Cavity pH at 280°C with Mississippi River Water Ingress

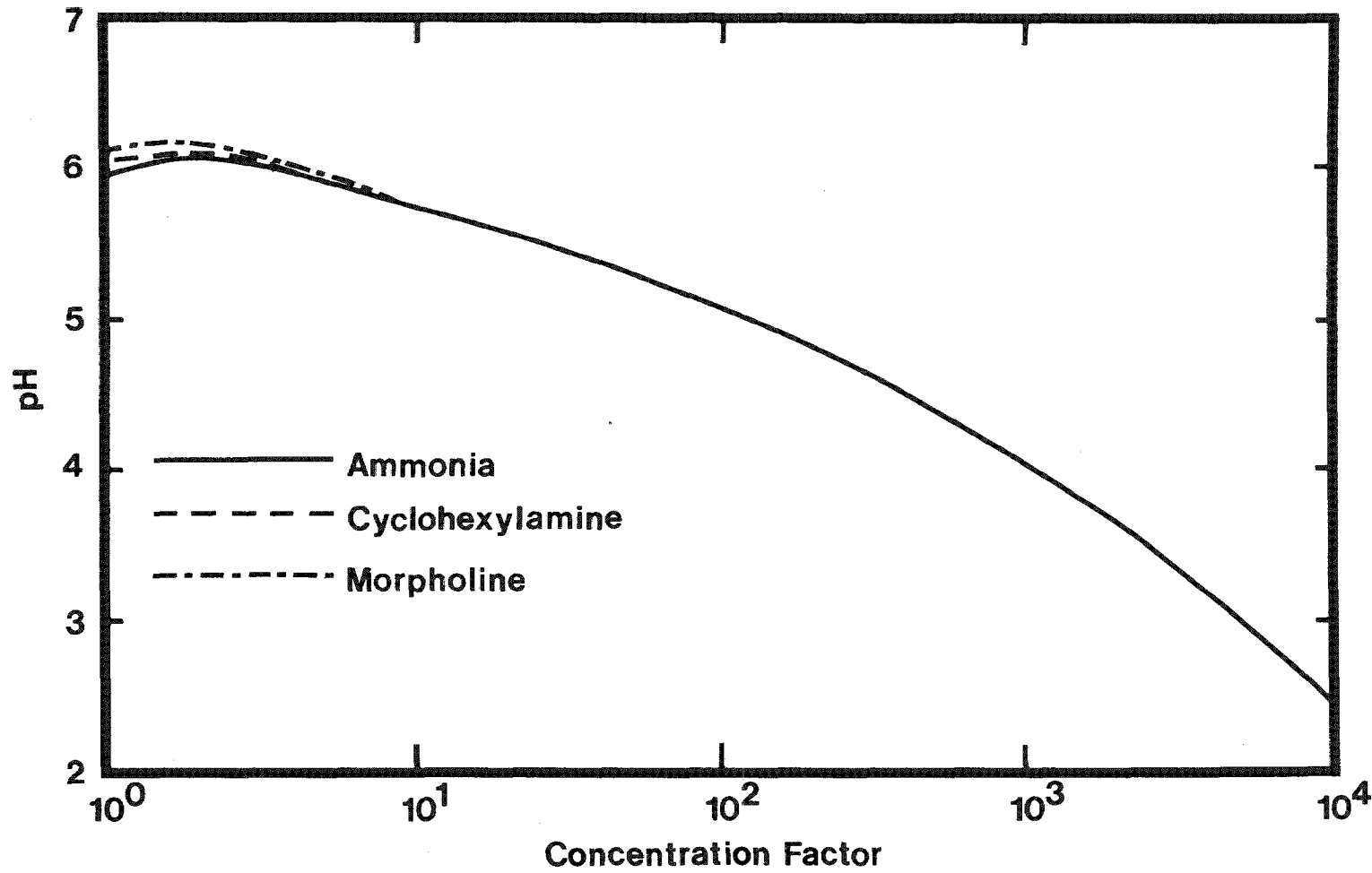


Figure 2-3. Effect of AVT Additives on Isolated Cavity pH at 280°C with Seawater Ingress

## DYNAMIC EQUILIBRIUM MODEL

### Model

Recognizing that the isolated cavity model was not applicable to describing the dynamic vapor to liquid equilibrium which exists in the steam generator bulk fluid as the coolant is boiled to higher qualities, a second model was developed. In this model, the steam produced remains in equilibrium with the residual liquid solution.

### Results

The predicted pH variation at 280°C in the bulk coolant is shown in Figures 2-4 and 2-5 for Mississippi River and seawater inleakage, respectively, as a function of local steam quality and designated amine. In general, pH decreases are predicted to occur in the bulk coolant with seawater ingress and pH increases with fresh water ingress. At low concentration factors, i.e., steam qualities up to 90%, the change in solution pH is considered to be of little consequence. At higher qualities, results given by the dynamic equilibrium and isolated cavity models are essentially the same. As such, additional consideration was not given to the dynamic equilibrium model.

### IMPLICATION OF RESULTS

It is recognized that significant inaccuracies can be present in the simplistic model and the physical chemistry parameters employed in the models. In addition, species interactions which are not recognized in the model could be occurring. In particular, reactions of silica, metal oxides, and metal were not considered in this phase of the model development. Nonetheless, certain general implications can be drawn from the results.

During condenser inleakage highly acidic solutions will be formed in plants using seawater and brackish coolants during the process of evaporation in regions where local evaporation of the bulk coolant to near dryness can occur. Some neutralization of these solutions could result from dissolution of metal oxides or metals surrounding or forming the cavity. In any event, the acidic solutions, generically hydrochloric acid, would be expected to lead to aggressive corrosion in such areas. That ferrous chloride solutions can lead to aggressive attack of carbon steel materials at steam generator temperatures has been demonstrated by Potter and Mann (7). In their experiments, the rapid growth of non-protective magnetite was observed in 0.1 molar ferrous chloride solutions

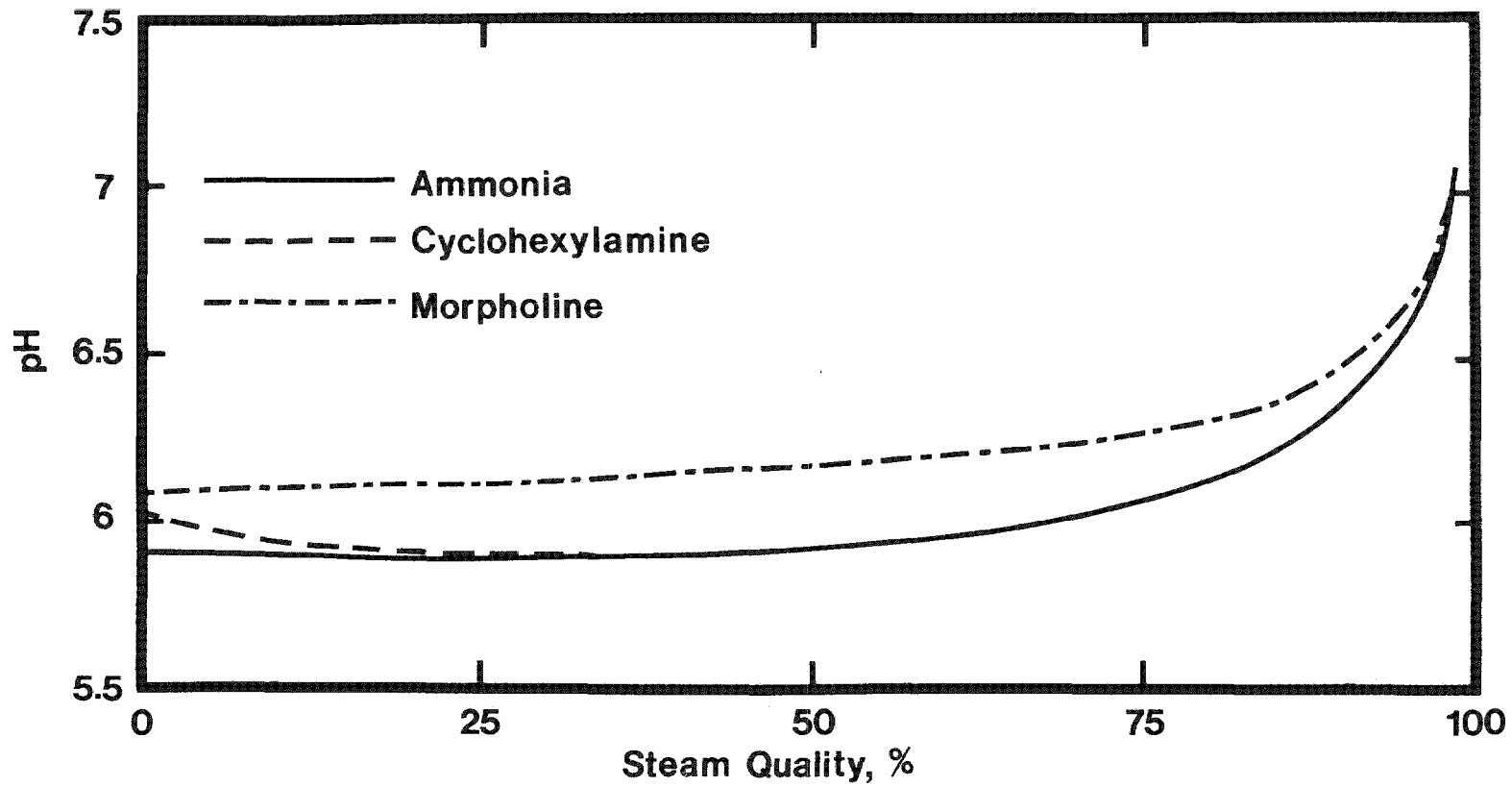


Figure 2-4. Effect of AVT Additives on Bulk Coolant pH at 280°C with Alkaline Fresh Water Ingress

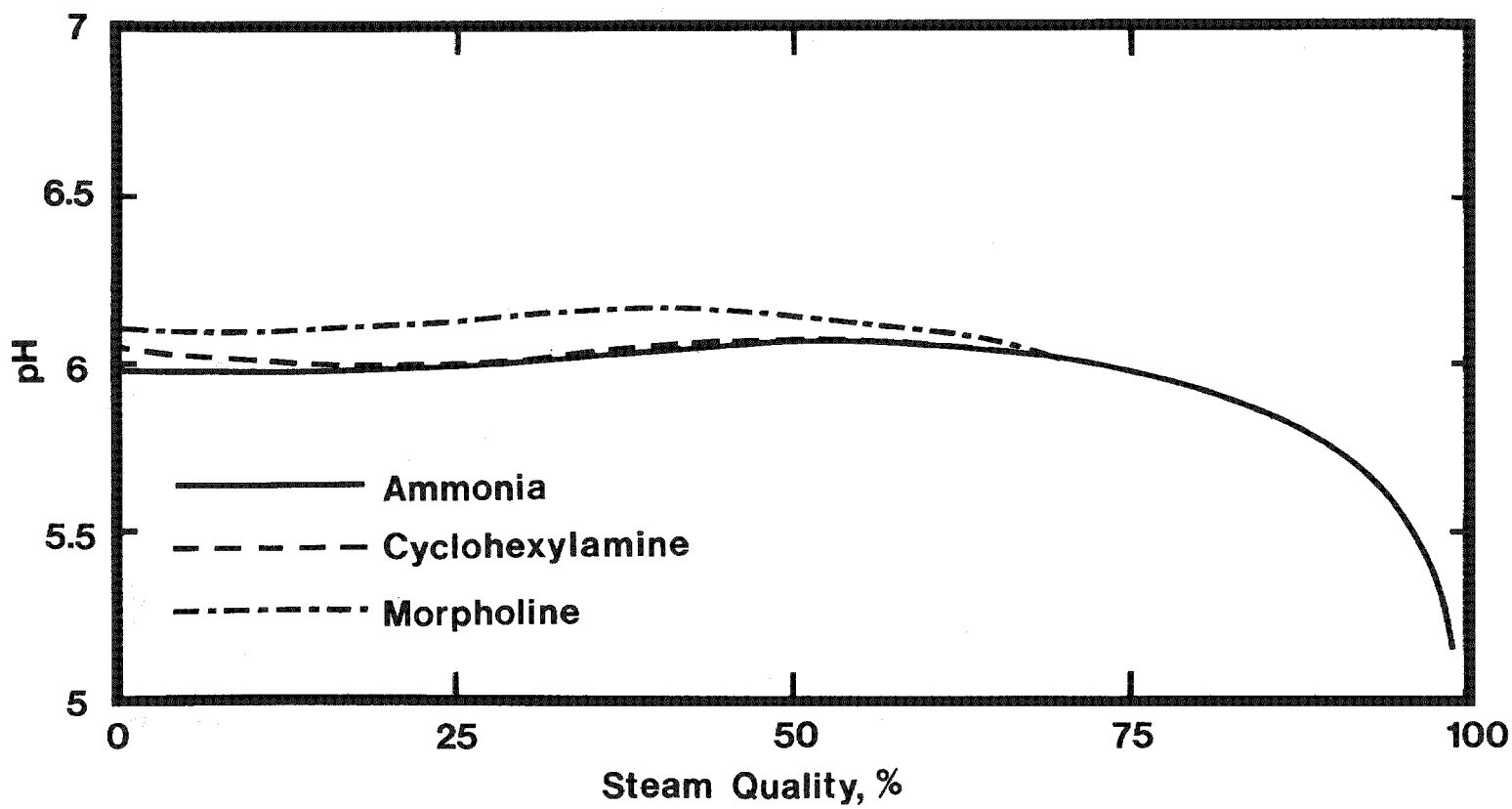


Figure 2-5. Effect of AVT Additives on Bulk Coolant pH at 280°C with Seawater Ingress

at 300°C. Ferrous chloride would be expected to result from corrosion of support plates where crevices are formed with the tubes if such crevices function even intermittently as isolated cavities.

In a cooling tower plant, the formation of sulfuric acid in local areas is expected. However, the local corrosion rate would not be expected to be as high as that for the seawater case in that similar concentrations of ferrous sulfate and ferrous chloride exhibit markedly different pH. For example, a 0.1 molar solution of ferrous chloride has a pH of approximately 3.0 at 300°C whereas that of a 0.1 molar solution of ferrous sulfate is approximately 5. Recognizing that salts of strong acids generally lead to corrosion rates similar to those of the strong acid itself at a similar pH (8), carbon steel corrosion in the chloride solution from seawater would be expected to be significantly more rapid than in the sulfate solution from the cooling tower water.

The predicted behavior of solution chemistry during ingress of Lake Michigan or Mississippi River water was nearly identical. Both waters would be expected to lead to pH elevations in an isolated cavity and in the bulk fluid as boiling progresses. At a concentration factor of 10,000, predicted sodium hydroxide concentrations were approximately 20 ppm and 60 ppm in the Lake Michigan and Mississippi River water cases, respectively. Significant corrosion of carbon steel is not expected at such concentrations (9). However, stress corrosion cracking of highly stressed Alloy 600 has been observed after less than 1,000 hours at a sodium hydroxide concentration of 0.4% at 350°C (10).

## Section 3

### SOLUTION CHEMISTRY IN THE PRESENCE OF SILICA

#### MODEL CONSIDERATIONS

Since 50 to 200 ppb silica is normally present in the steam generator blowdown even in the absence of significant condenser inleakage, consideration of the effect of a background silica level on solution chemistry during inleakage was mandatory. To model the effect of silica, it was necessary to consider the presence in solution of silicic acid ( $H_4SiO_4$ ) and its anions  $Si(OH)_5^-$  and  $Si(OH)_6^-$  in addition to those species addressed in Section 2.

Because of the major effect that inclusion of each precipitating species has on the complexity of the solution chemistry model, an extensive review of possible silica precipitates was dictated. At the request of NWT (through EPRI), available thermodynamic data for major silica compounds in the temperature range of interest were analyzed at San Diego State (11). Free energies of reactions and, where appropriate, equilibrium constants for 25 reactions involving quartz and iron-, magnesium-, and calcium-containing silica compounds were developed (11). Information was derived for additional reactions by judicious combination of the reported reactions. For example, the solubility product for serpentine at 275°C was derived (Appendix B).

Analysis of the thermodynamic data indicated that silica and five calcium- and magnesium-containing silicates were likely precipitates from the aqueous solutions of interest. This dictated that nine possible precipitates be considered in the models, i.e., silica, five calcium and magnesium silicates, calcium and magnesium hydroxides, and calcium sulfate.

Because a comprehensive treatment of the nine precipitates would necessitate consideration of 512 sets of simultaneous equations, it was deemed advisable to seek an alternative approach to computer solution of the model. Review of The Free-Energy Minimization Method (12) used for the calculation of complex chemical reactions in the gaseous phase disclosed no advantage of this method compared to the equilibrium constant method.

To facilitate the modeling effort, a phase diagram for the relative stabilities of the nine possible precipitates was constructed (Figure 3-1) as a function of the  $Mg^{++}/Ca^{++}$  ratio and the silicic acid concentration in solution, with the  $SO_4^{=}/(OH^-)^2$  ratio as parameter. Although not specifically identified in Figure 3-1, consideration is given to  $CaSO_4$  by referencing the  $SO_4^{=}/(OH^-)^2$  parameter. This phase diagram was used to develop computer programs tailored to specific cases at hand rather than address the general problem by the original techniques, i.e., solutions of 512 sets of simultaneous equations. Construction of such phase diagrams is described in Appendix C.

The method for developing specific computer programs consists of locating on the phase diagram the initial location of the aqueous system expressed by the ratio  $Mg^{++}/Ca^{++}$  and the silicic acid concentration. From this location and the ratio  $SO_4^{=}/(OH^-)^2$ , possible precipitates in equilibrium with the liquid phase are determined thus establishing the set of equations to be solved (out of 512 sets of equations). As steam quality is increased, the progression of the aqueous system on the phase diagram indicates which set of equations must be considered. Computer programs tailored on the basis of such information are simplified considerably compared to a general program for all cases.

Using this technique, one program was tailored for the isolated cavity model for condenser inleakage of seawater, brackish water and cooling tower water. Another program was written for condenser leakage of Mississippi River and Lake Michigan water.

The solubilization reaction and corresponding equilibrium relation of fourteen compounds initially considered for possible precipitation are listed in Table C-1 of Appendix C. The solubility products for calcium and magnesium hydroxides and for calcium sulfate were calculated as functions of temperature using the constants of Table A-1 of Appendix A. The other solubility products,  $K_s$ , are calculated from the solubilization free energies,  $\Delta G^\circ$ , at temperature T as follows:

$$\log K_s = (\ln K_s)/2.3 = -\Delta G^\circ/2.3 RT \quad (3-1)$$

$\Delta G^\circ$  for each solubilization reaction of the silicate compounds was derived using the procedure illustrated in Appendix B.

Figure 3-1 presents the phase diagram for the nine precipitable compounds and the paths for the cases of seawater and Mississippi River water coolants. Distinct

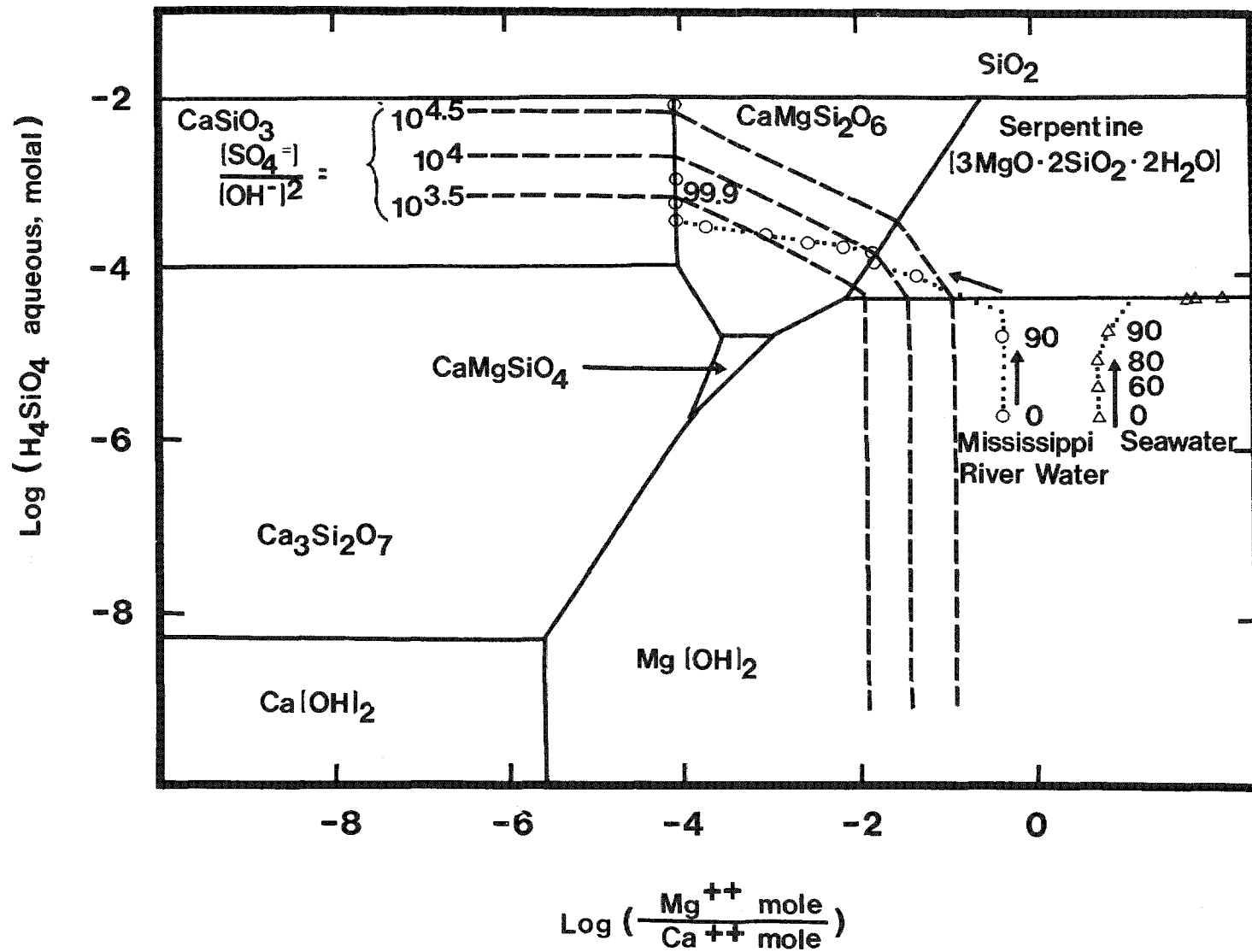


Figure 3-1. Phase Diagram of Relative Stabilities at 275°C

regions of precipitate stability are shown for all compounds of pertinence other than  $\text{CaSO}_4$ . In the selected phase diagram, a distinct region of  $\text{CaSO}_4$  stability cannot be defined in that precipitation of this compound can occur simultaneously with any of the other compounds depending on the  $[\text{SO}_4^{=}/\text{OH}^{-2}]$  ratio.

The other five silicates have no domain of stability in equilibrium with the aqueous solution at 275°C, based on the free energies of Table C-2 of Appendix C.

#### MODELING RESULTS

The predicted variation in solution pH is shown in Figure 3-2 for Mississippi River water inleakage as the solution is boiled in an isolated cavity. The neutral pH variation also is shown for reference. Initial solution concentrations were identical to those of Section 2 other than for the addition of silica. Calculations are terminated when the concentrated solution boiling temperature equals the tube wall temperature, approximately corresponding to a 10°C solution boiling point elevation.

It should be noted that the definition of pH used in the present study is that followed by Mesmer (13) in the determination of the dissociation constant of water at high temperature, i.e., the negative of the logarithm of the hydrogen ion concentration (not of its activity). Similarly, neutral pH is defined as that pH where the hydrogen and hydroxyl ion concentrations are equal. The neutral pH is a function of ionic strength. Therefore, the variation of pH for concentrated solutions must be considered in relation to the variation of the neutral pH to obtain an indication of the acidity or basicity of the solution. In Figure 3-3, for example, it is seen that the hydroxyl ion concentration above that present at neutral pH is increasing monotonically with the concentration factor for Mississippi River water in the absence of silica, even while the pH decreases at concentration factors above approximately  $10^5$ , as seen in Figure 3-2.

As shown, the model predicts that in a cavity with fresh water ingress, the hydroxyl ion reaches a concentration of about 0.1 molal in the absence of initial silica. This corresponds to a sodium hydroxide concentration of 0.4% and a room temperature pH of 13. Inconel is subject to stress corrosion cracking at such concentrations (10).

Worthy of notice is the predicted effect of 100 ppb silica as shown in Figure 3-3, i.e., a 100 ppb bulk water silica concentration reduces the hydroxyl concentration

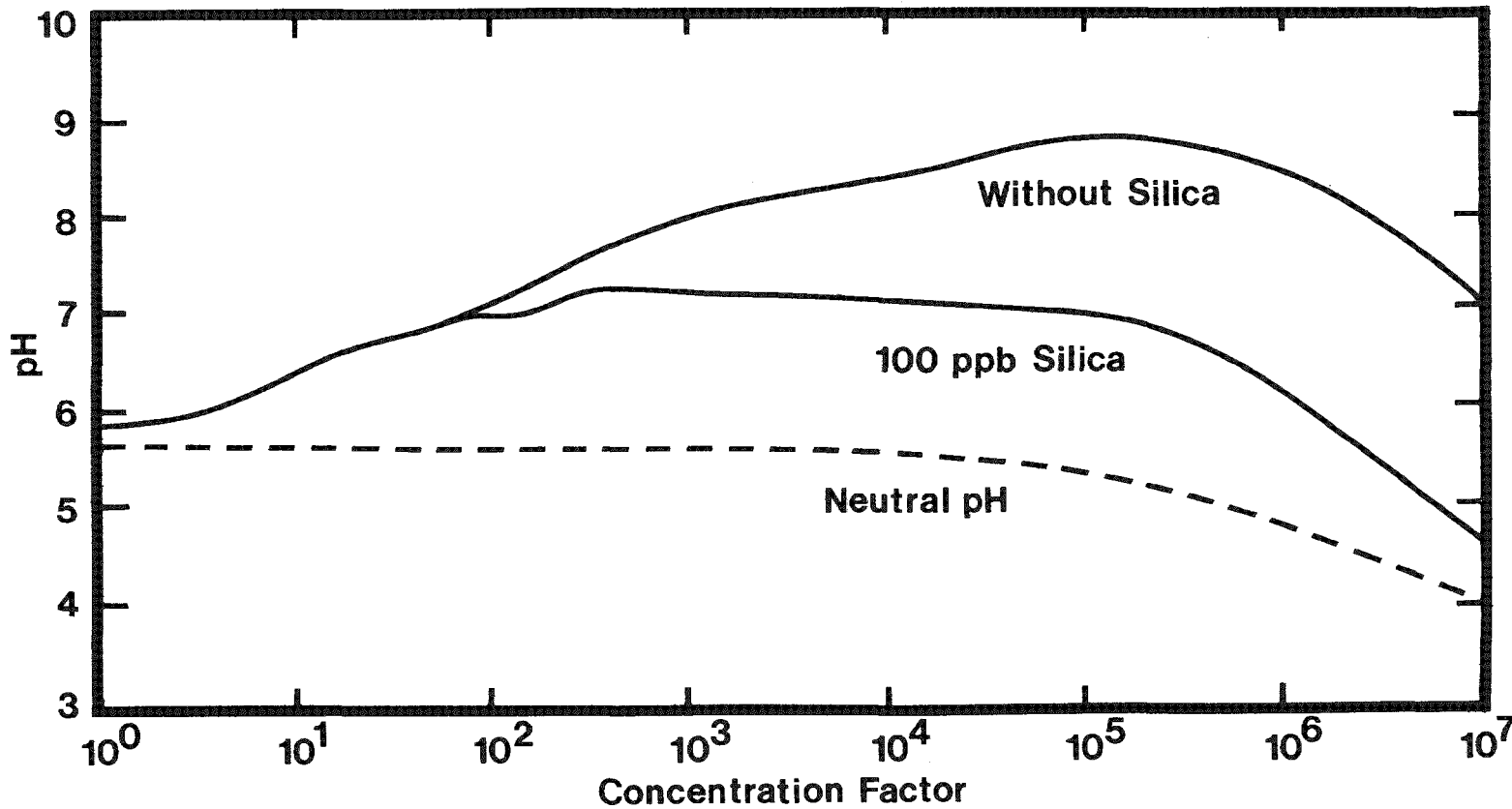


Figure 3-2. Variation of Isolated Cavity pH with Mississippi River Water Ingress at 280°C

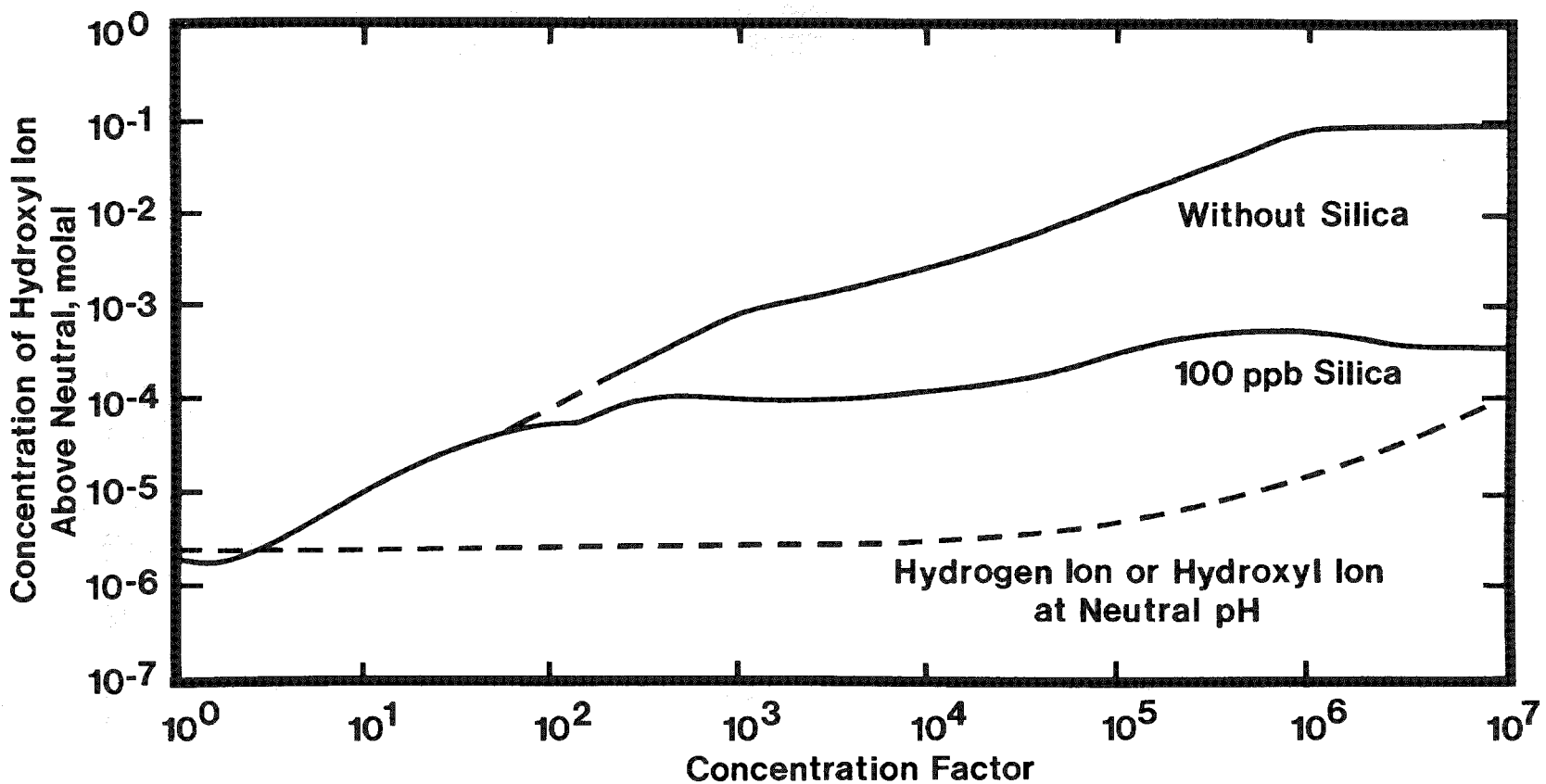
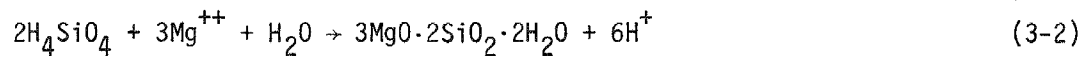


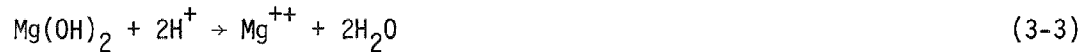
Figure 3-3. Variation of Hydroxyl Ion Concentration in an Isolated Cavity with Mississippi River Water Ingress at 280°C

in the cavity significantly as boiling progresses. Higher silica levels have no further effect at the selected Mississippi River water inleakage rate because the precipitation of silica ( $\text{SiO}_2$ ) limits its concentration in solution.

No appreciable effect on pH of 100 ppb silica was found in the isolated cavity for seawater, brackish water and cooling tower water coolants at the initially selected leak rate of 5 liters/h at concentration factor up to ten thousand (Figure 3-4). This can be understood by considering the acidic solution in equilibrium with magnesium hydroxide and/or calcium sulfate obtained initially without silica, and adding silicic acid ( $\text{H}_4\text{SiO}_4$ ). The acidity produced by precipitation of serpentine



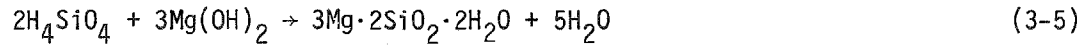
is compensated by redissolution of magnesium hydroxide



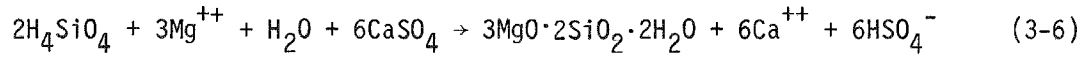
and/or calcium sulfate



The net result can be considered to be a reaction of silicic acid with magnesium hydroxide



and/or with calcium sulfate



Such reactions have no pH effect as long as the magnesium hydroxide and/or calcium sulfate precipitate remains in equilibrium with the aqueous solution.

At sufficiently high silica levels, available magnesium hydroxide and/or calcium sulfate precipitates could be exhausted. If this occurs, further silica precipitation could decrease solution pH as is the case for 200 ppb silica (Figure 3-4).

In initially assessing the effect of cooling water contaminants, a 5 liter/h leak rate was assumed. In such cases, the chloride to silica ratios in the

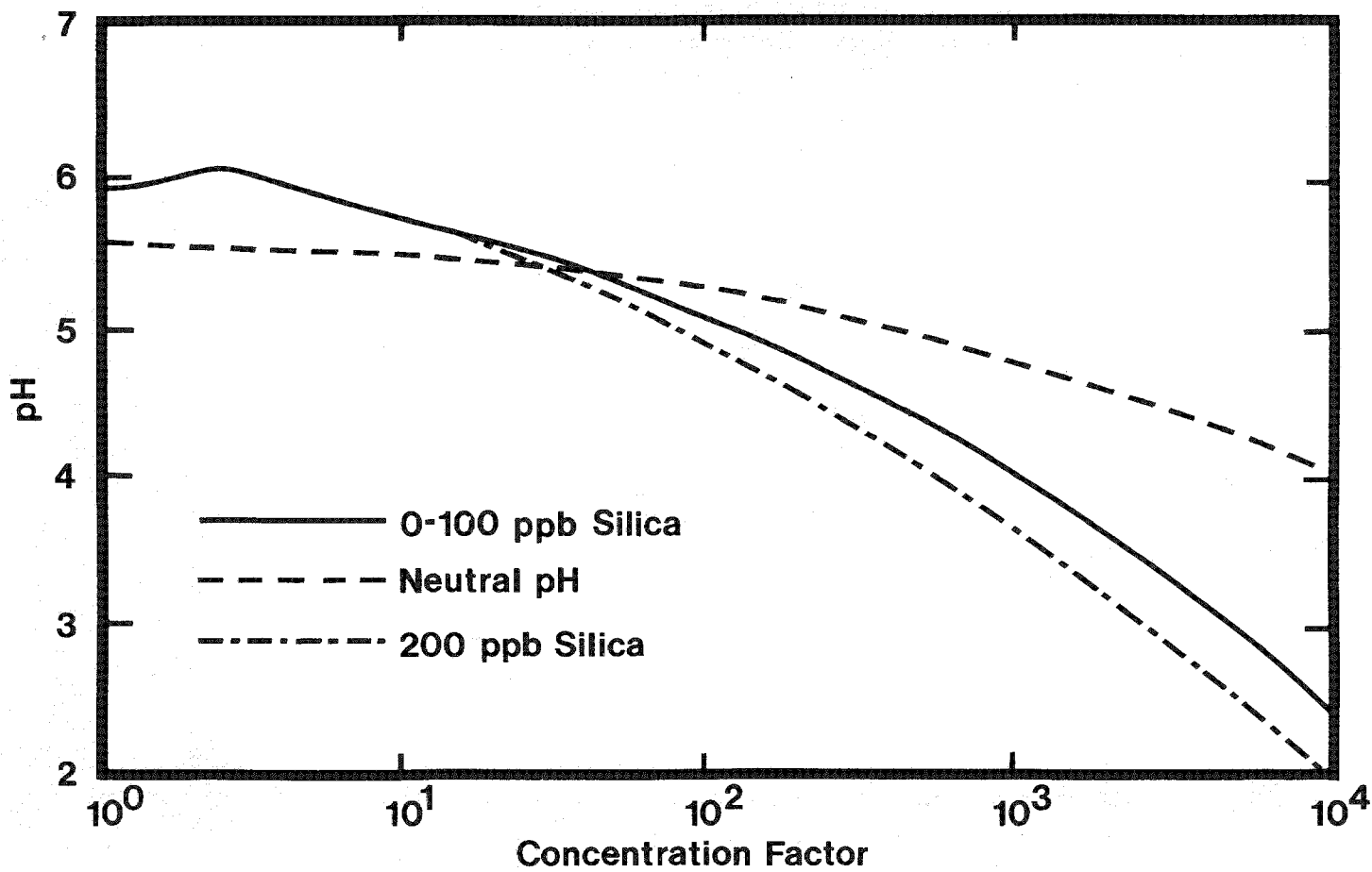


Figure 3-4. Variation of Isolated Cavity pH with Seawater Ingress at 280°C

boiler water are much larger than those expected with good operation (as defined below). Since lower ratios are considered to reflect more accurately condenser leakage control currently practiced at most seawater sites, additional calculations were performed for the case where condenser leakage in a seawater cooled plant was controlled to limit blowdown chloride to 50 ppb (assuming negligible hideout). This corresponds to a 0.036 liter/h (0.00015 gpm) condenser leak at a blowdown of 13620 liters/h (60 gpm).

Results are shown in Figure 3-5. As expected, the effect of silica on crevice pH is more marked. In addition, the effect at the higher concentration factors is the same for 10 and 200 ppb silica. This behavior results from silica precipitation as it saturates the cavity solution.

There is no appreciable difference in results obtained with the dynamic equilibrium and isolated cavity models above 90% steam quality. In particular, the results of Figure 3-2 through 3-5 also represent the model prediction for the pH variation of steam generator bulk water as steam quality increases above 90% along the length of the generator.

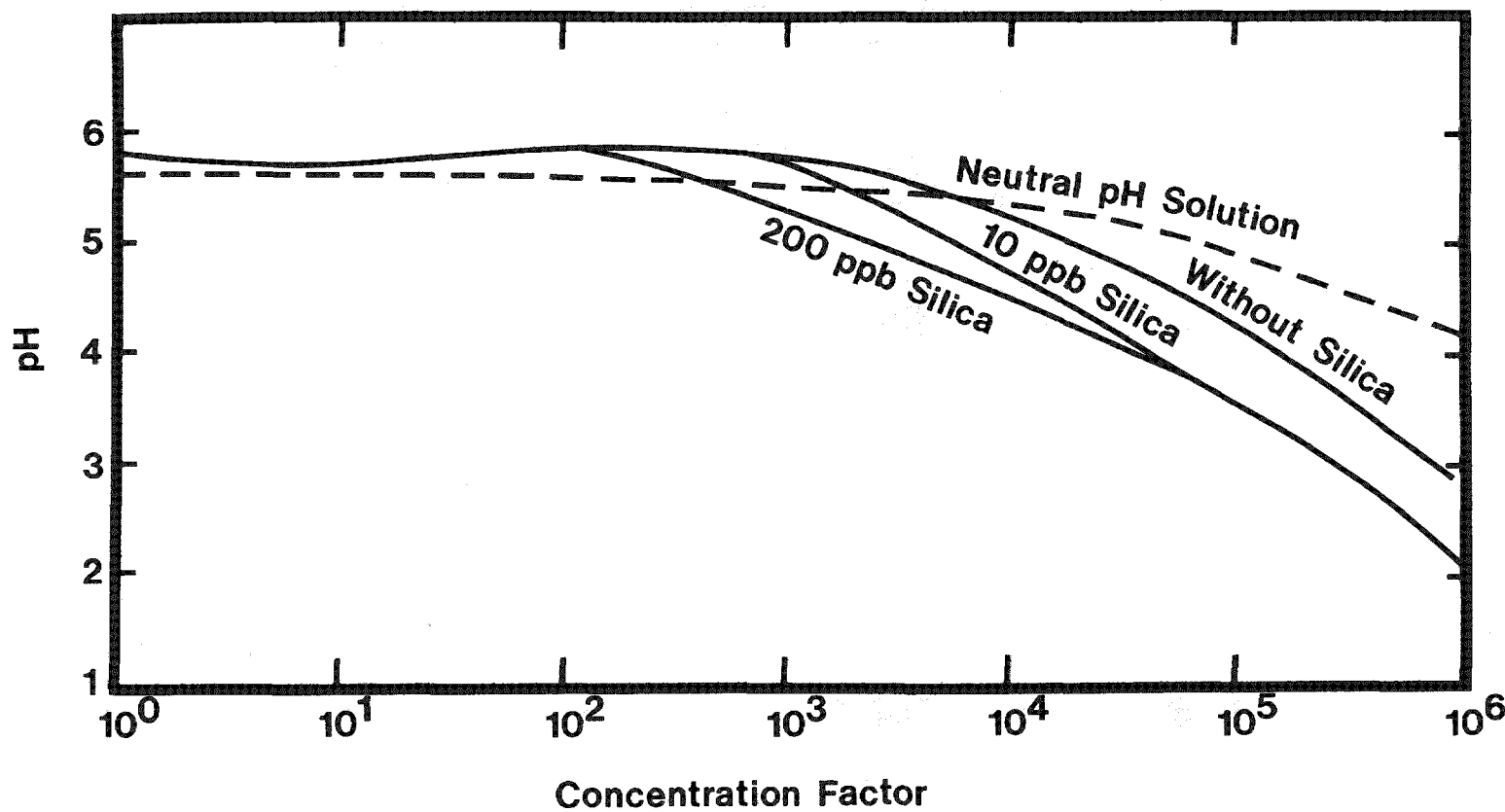


Figure 3-5. The Effect of Silica on the Variation of Isolated Cavity pH with Concentration Factor  
(Temperature at 280°C; Seawater Inleakage to give 50 ppb in Steam Generator)

## Section 4

### IMPLICATIONS OF MODELING RESULTS

The following conclusions can be developed from the modeling studies:

1. Acidic solutions (HCl) will be formed in crevices of operating PWR steam generators during periods of condenser cooling water inleakage at seawater and brackish water sites. Crevice pH at operating temperatures will be 2 to 3 units below neutral at concentration factors of  $10^4$  to  $10^6$  above the bulk coolant.
2. Acidic solutions ( $H_2SO_4$ ) will be formed in crevices at cooling tower sites where sulfuric acid is employed to control condenser scaling.
3. The presence of 10 to 100 ppb silica in the boiler water will reduce crevice pH below that calculated considering only seawater ingress when bulk water chloride solutions are near normal operating levels of 50 ppb.
4. Caustic solutions with NaOH strengths approaching 0.1 Molal can be generated in crevices at fresh water sites in the absence of background silica contamination in the boiler water. With 100 ppb silica present in the boiler water, crevice pH is reduced by the precipitation of silica compounds. As such, silica could be beneficial in minimizing crevice pH excursions during cooling water inleakage at fresh water sites.

Assuming a crevice concentration factor of 10,000 above the bulk water, the modeling results can be employed to qualitatively assess the impact on crevice pH of cooling water inleakage rate as shown in Figure 4-1. As shown, the pH depression below neutral pH in the crevice is several tenths of a unit or less at blowdown chloride concentrations below 100 ppb. However, the acid side depression at 1 ppm chloride is a full unit and at 10 ppm is 1.6 units.

Accepting the relation between carbon steel corrosion rates and pH at 300°C published by Mann (14), a relation between estimated carbon steel corrosion rate and blowdown chloride level at seawater sites can be developed as shown in Figure 4-2.

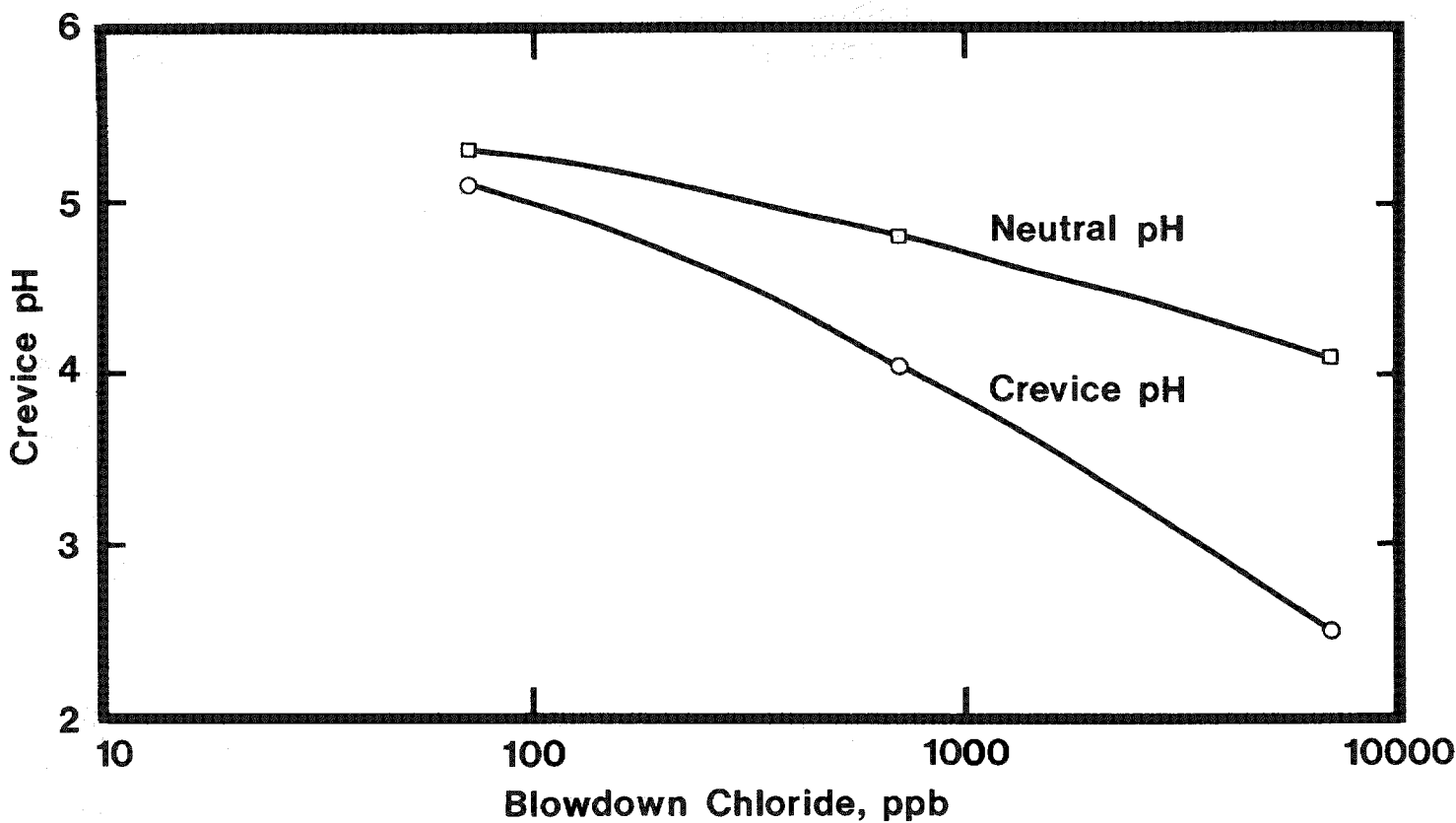


Figure 4-1. Predicted Crevice pH at a Seawater Plant (Concentration Factor = 10,000)

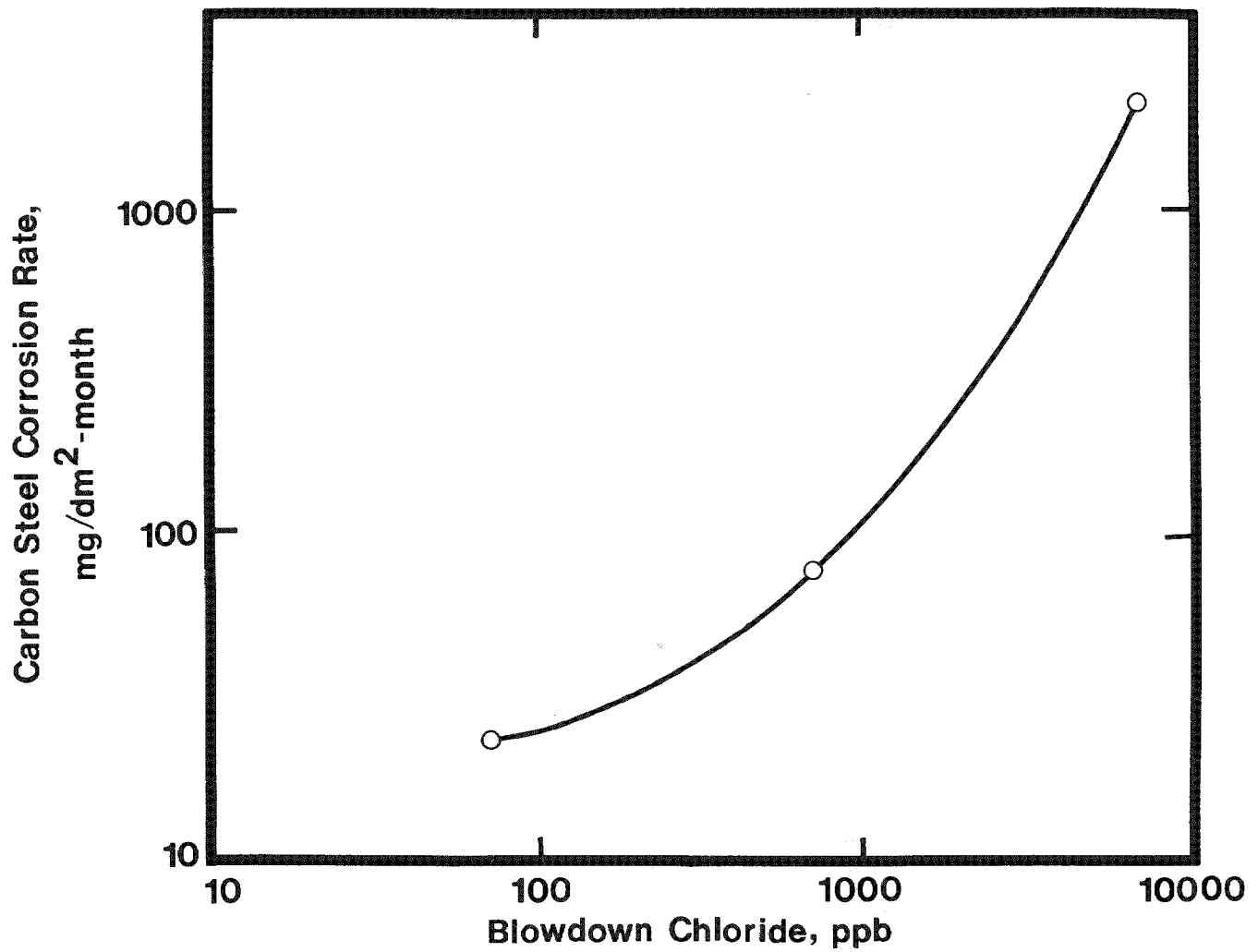


Figure 4-2. Tube Support Plate Corrosion Rate at Seawater Cooled Plant (Concentration Factor = 10,000)

Finally, the time to detectable denting assuming no crevice oxide loss or compressibility can be approximated as shown in Figure 4-3.

Based on a relation such as Figure 4-3, plant operators could assess the impact of any long term operating strategy relative to the initiation and propagation of denting.

Obviously the above treatment is simplistic but it serves to illustrate the final goal of the overall modeling effort, i.e., the development of plant operating guidelines to increase the probability of long term steam generator integrity. Many deficiencies in the model and the corrosion data base necessary for its ultimate application are recognized by the authors. To address some of the modeling concerns, an extensive modeling effort under EPRI Project S167-1 recently has been funded.

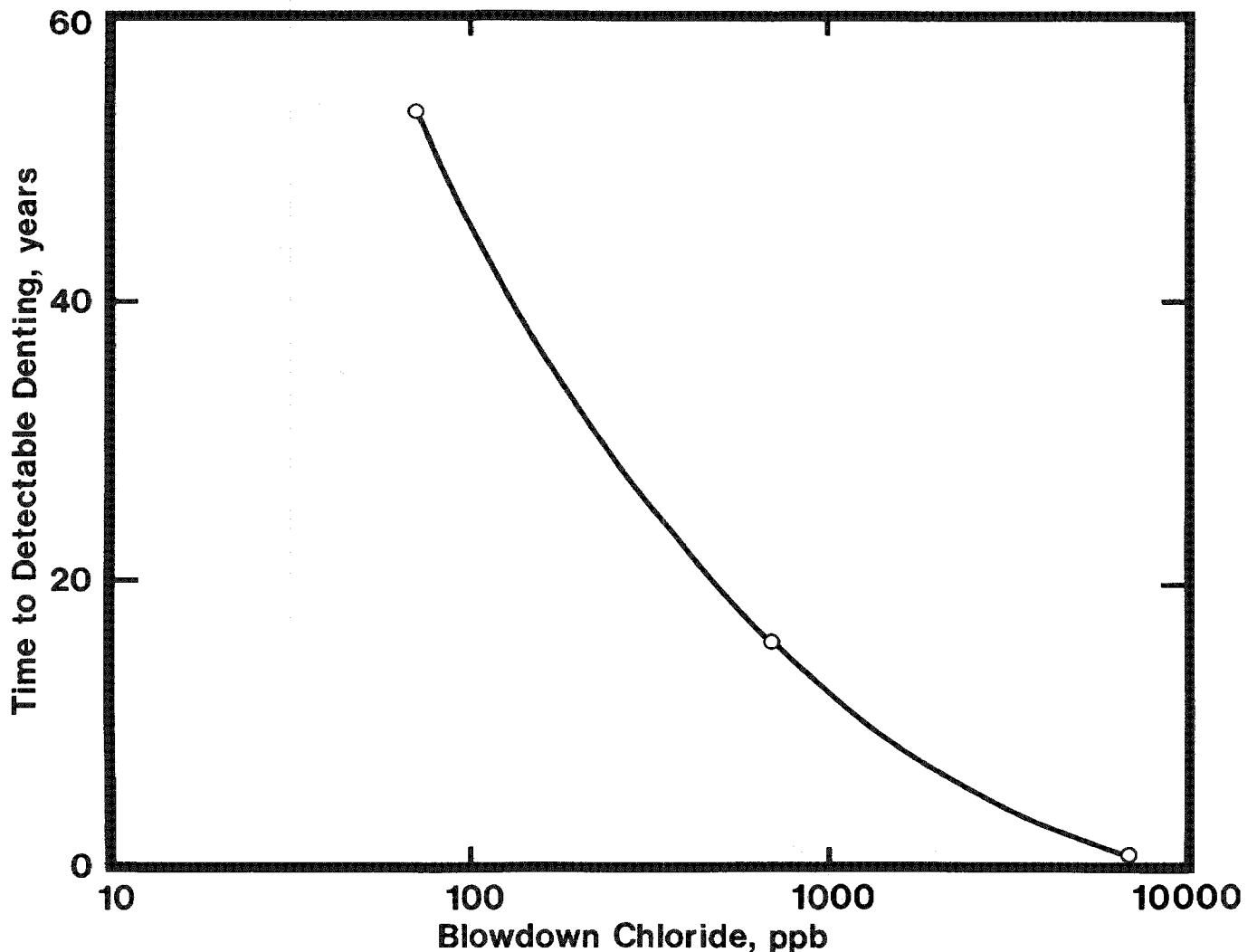


Figure 4-3. Effect of Blowdown Chloride Concentration on Denting at a Seawater Plant  
(Concentration Factor = 10,000)

## Section 5

### FUTURE EFFORTS

Under EPRI RP404-1 and the initial stages of S167-1, a general computer program has been developed for up to three precipitable compounds: calcium sulfate, calcium hydroxide and magnesium hydroxide. The modeling approach subsequently was modified to allow inclusion of silica and silicate compounds (nine possible precipitates). Future modeling efforts will be undertaken in the S167 project. Such efforts initially are being focused on expanding the phase diagram method to include iron interactions.

Simultaneously, steady state and transient crevice concentration factor estimates are being developed considering diffusion and thermal hydraulics of the crevices. Electrochemical effects on solution chemistry in the tube to tube support plate crevice and the attendant effect on the corrosion process also are being considered.

Employing estimates of crevice solution pH developed from the augmented model, and laboratory and operating plant corrosion observations at given chemistry conditions, more reliable plant operating guidelines (e.g., Figure 4.3) will be established. Subsequent to establishing these guidelines, the specific goal of S167-1 is to demonstrate a viable technique of achieving the necessary chemistry control with emphasis on the application of full flow condensate polishing.

## REFERENCES

1. Katkovskaya, K. Ya., Vaineikis, A. S., and Dubrovskii, I.Y., "The Effect of Temperature on the pH Value of the System  $H_2O-CO_2-NH_3$ ", *Teploenergetka*, 21, No. 7, pp. 8-10 (1974).
2. Cohen, P., "The Chemistry of Water and Solution at High Temperature for Application to Corrosion in Power Systems", presented at the Seminar on Chemistry and Aqueous Corrosion in Steam Generators, Ermenonville, France, March 13-17, 1972.
3. Pocock, F. S., "Control of Iron Pickup in Cycles Utilizing Carbon Steel Feedwater Heaters", *Proc. Amer. Power Conf.*, 28, pp. 758-71 (1966).
4. Samuel, T., "Thermal Stability of Cyclohexylamine and of Morpholine", Centre Belge D'Etude et de Documentation des Eaux, January 1955, pp. 2-3 (in French).
5. Albrecht, S. H. and Schuck, J. J., "Laboratory Evaluation of Neutralizing Amines for Use in Steam Systems", *Materials Performance*, 15, No. 3, pp. 23-25, March 1976.
6. Mesmer, R. E., Hitch, B. F., and Herting, D., "High-Temperature Equilibria in Light and Heavy Water", in *Chemistry Division Annual Progress Report*, period ending May 20, 1974, Oak Ridge National Laboratory, pp. 82-83 (ORNL-4976).
7. Potter, E. C. and Mann, G. M. W., "The Fast Linear Growth of Magnetite on Mild Steel in High-Temperature Aqueous Conditions", *British Corrosion J.*, 1, pp. 26-35 (1965).
8. Uhlig, H. H., "Corrosion and Corrosion Control", John Wiley, New York, 1967, p. 100.
9. *Ibid*, p. 85.
10. Berge, Ph., Donati, J. R. and Villard, D., "Caustic Stress Corrosion of Austenitic Fe-Cr-Ni Alloys", Sixth International Congress on Metallic Corrosion, Sydney, December 1975.
11. Murray, R. C. and Cobble, J. W., Appendix C in "Chemical Thermodynamic Studies of Aqueous Trace Components in Light Water Reactors at High Temperature and Pressure, Annual Report for the period March 1, 1976 through December 31, 1976", J. W. Cobble, Ed., San Diego State University Foundation, March 15, 1977.
12. Zeleznik, F. J. and Gordon, S., "Calculation of Complex Chemical Equilibria", *Applied Thermodynamics*, American Chemical Society Publications, 1968.

13. Mesmer, R. E., Baes, C. F., Jr., and Sweeton, F. M., "Boric Acid Equilibria and pH in PWR Coolants", Proc. of the 32nd Intl. Water Conf., Pittsburgh, pp. 55-65 (1971).
14. Mann, G. M. W., "History and Causes of On-Load Waterside Corrosion in Power Boilers", Combustion, August 1978, pp. 28-37.

## Appendix A

### DERIVATION OF GOVERNING RELATIONS IN THE ABSENCE OF SILICA

#### NOMENCLATURE AND GENERAL RELATIONS

Nomenclature is summarized at the end of this appendix. In the following discussion,  $\emptyset$ ,  $B_1$ ,  $S_1$ ,  $S_2$ ,  $H_1$ ,  $L_1$ ,  $N$ ,  $C$  and  $M$  represent the concentrations in solution of ions  $\text{OH}^-$ ,  $\text{NH}_4^+$ ,  $\text{HSO}_4^-$ ,  $\text{SO}_4^=$ ,  $\text{HCO}_3^-$ ,  $\text{Cl}^-$ ,  $\text{Na}^+$ ,  $\text{Ca}^{++}$ , and  $\text{Mg}^{++}$ , respectively. Because the carbonate species disappear very early in the process by volatilization of carbon dioxide when the solution pH is close to neutral, the concentration of  $\text{CO}_3^=$  is negligible.

$X_1$ ,  $X_2$  and  $X_3$  represent the amounts, if any, of precipitates  $\text{CaSO}_4$ ,  $\text{Ca}(\text{OH})_2$  and  $\text{Mg}(\text{OH})_2$  respectively, in mole per kg of solution (from which it precipitates out). The variations of solution density with composition are neglected.

$S_0$  represents the total amount of bisulfate and sulfate including the amount in the  $\text{CaSO}_4$  precipitated,  $C_0$  the total amount of calcium including the amount in the  $\text{CaSO}_4$  and the  $\text{Ca}(\text{OH})_2$  precipitated, and finally  $M_0$  the total amount of magnesium including the amount in the  $\text{Mg}(\text{OH})_2$  precipitated.

The mass conservation relations for calcium, sulfur, and magnesium are as follows:

$$C + X_1 + X_2 = C_0 \quad (A-1)$$

$$S_1 + S_2 + X_1 = S_0 \quad (A-2)$$

and

$$M + X_3 = M_0 \quad (A-3)$$

Solubility products, when applicable, can yield up to three equations:

$$C * S_2 = K_6 \quad (A-4)$$

$$C * \emptyset^2 = K_4 \quad (A-5)$$

$$M * \emptyset^2 = K_3 \quad (A-6)$$

The sulfate-bisulfate equilibrium can be expressed as:



for which the equilibrium constant is written as:

$$\varnothing * S1/S2 = K5 \quad (A-8)$$

The ionic product for water is:

$$[H^+] * \varnothing = K1$$

from which

$$[H^+] = K1/\varnothing \quad (A-9)$$

The solution electroneutrality condition yields:

$$A + (2 * C) + (2 * M) + K1/\varnothing - \varnothing - 2 (S1 + S2) + S1 = 0 \quad (A-10)$$

where A is defined as:

$$A \equiv N + B1 - L1 - H1 \quad (A-11)$$

Table A.1 lists pertinent equilibrium constants as functions of temperature and ionic strength.

#### CASE (1), NO PRECIPITATE

In the case of no precipitation, Eq. A-4, 5 and 6 are inapplicable. Instead, the following inequalities apply:

$$C * S2 < K6 \quad (A-1-1)$$

$$C * \varnothing^2 < K4 \quad (A-1-2)$$

and

$$M * \varnothing^2 < K3 \quad (A-1-3)$$

Also,

$$X1 = X2 = X3 = 0 \quad (A-1-4)$$

Substituting these values in Eq. A-1, 2 and 3

$$C = C0 \quad (A-1-5)$$

$$S1 + S2 = S0 \quad (A-1-6)$$

$$M = M0 \quad (A-1-7)$$

Eq. A-8 and the electroneutrality equation A-10 are valid for all cases. From Eq. A-1-6:

$$S1 = S0 - S2 \quad (A-1-8)$$

Table A-1  
PHYSICAL CHEMISTRY RELATIONS\*

$$\begin{aligned}
 \log [H^+] [OH^-] &= -151.713/T - 111.491 - 0.03685 T + 44.077 \log T + \\
 &\quad 2A\sqrt{I}/(1 + \sqrt{I}) - (0.6356 - 0.001078 T) I \\
 \log ([NH_4^+] [OH^-]/[NH_4OH]) &= -0.000028 T^2 + 0.018T - 7.63 + A\sqrt{I}/(1 + 1.5\sqrt{I}) \\
 \log [Ca^{++}] [OH^-]^2 &= -25.7085 + 12.9722 \log T - 530.49/T - 0.032331 T + \\
 &\quad 6A\sqrt{I}/(1 + B\sqrt{I}) - CI - DI^2 \\
 \log [Mg^{++}] [OH^-]^2 &= \log [Ca^{++}] [OH^-]^2 - 5.6 \\
 \log ([H^+] [SO_4^{=}]/[HSO_4^-]) &= 91.471 - 33.0024 \log T - 3520.3/T + 4A\sqrt{I}/(1 + E\sqrt{I}) \\
 \log [Ca^{++}] [SO_4^-] &= -133.207 + 53.5472 \log T + 3569.6/T - 0.0529025 T + \\
 &\quad 8A\sqrt{I}/(1 + 1.5\sqrt{I}) \\
 \log ([H^+] [HCO_3^-]/[H_2CO_3]) &= -2382.2/T + 8.153 - 0.02194 T
 \end{aligned}$$

where the brackets indicate molal concentrations, I is the ionic strength, T (°K) the absolute temperature and:

$$A = 1.64189 - 0.015632 T + 6.32 \times 10^{-5} T^2 - 1.0626 \times 10^{-7} T^3 + 7.4661 \times 10^{-11} T^4$$

$$B = 0.473 + 0.00423 T - 3.916 \times 10^{-9} T^3$$

$$C = 0.362 - 0.002223 T + 3.29 \times 10^{-6} T^2$$

$$D = -0.0298 + 0.0001665 T - 2.38 \times 10^{-7} T^2$$

$$E = -0.866 + 0.00639 T - 9.6 \times 10^{-12} T^4$$

\*Carbonic acid data from Reference (1); remaining relations from Reference (2)

Substituting into Eq. A-8

$$\varnothing * (S_0 - S_2) / S_2 = K_5$$

from which

$$S_2 = \varnothing * S_0 / (\varnothing + K_5) \quad (A-1-9)$$

Substituting into Eq. A-1-8:

$$S_1 = S_0 - S_2 = K_5 * S_0 / (\varnothing + K_5) \quad (A-1-10)$$

Substituting for C, M, (S<sub>1</sub> + S<sub>2</sub>) and S<sub>1</sub> from Eq. A-1-5, A-1-7, A-1-6 and A.1.10, respectively, into the electroneutrality equation A.10 yields:

$$A + 2 * (C_0 + M_0 - S_0) + K_1 / \varnothing - \varnothing + K_5 * S_0 / (\varnothing + K_5) = 0 \quad (A-1-11)$$

Solution of Eq. A-1-11 yields the value for  $\varnothing$ . The pH of the solution is then:

$$P_1 = - \log (K_1 / \varnothing) \quad (A-1-12)$$

#### CASE (2), CALCIUM SULFATE PRECIPITATION

In the situation where only calcium sulfate precipitates, Eq. A-5 and A-6 are inapplicable. Instead, inequalities A-1-2 and A-1-3 apply. Also

$$X_2 = X_3 = 0 \quad (A-2-1)$$

and substituting these values in Eq. A-1 and A-3:

$$C + X_1 = C_0 \quad (A-2-2)$$

$$M = M_0 \quad (A-2-3)$$

Eq. A-2 and A-4 remain valid in the present case. As previously noted, Eq. A-8 and the electroneutrality equation A-10 remain valid in all cases.

Eliminating X<sub>1</sub> between Eq. A-2 and A-2-2 yields:

$$S_1 + S_2 = S_0 - C_0 + C \quad (A-2-4)$$

From Eq. A-4 and A-8 respectively:

$$S_2 = K_6 / C \quad (A-2-5)$$

and

$$S_1 = (K_5 / \varnothing) * S_2 = (K_5 / \varnothing) (K_6 / C) \quad (A-2-6)$$

Substituting into the electroneutrality equation A-10 for  $M$ ,  $(S1 + S2)$  and  $S1$ , from Eq. A-2-3, A-2-4, and A-2-6, respectively, yields:

$$A + 2 * (C0 + M0 - S) + K1/\emptyset - \emptyset + (K5/\emptyset) (K6/C) = 0 \quad (A-2-7)$$

A second equation between the two unknowns  $C$  and  $\emptyset$  is obtained by substituting for  $S2$  and  $S1$  from Eq. A-2-5 and A-2-6, respectively, into Eq. A-2-4

$$C^2 + (S0 - C0) * C - (1 + K5/\emptyset) * K6 = 0 \quad (A-2-8)$$

Simultaneous solution of Eq. A-2-7 and A-2-8 yields the values for  $C$  and/or  $\emptyset$ . The pH is then expressed by Eq. A-2-12.

### CASE (3), CALCIUM HYDROXIDE PRECIPITATION

With only calcium hydroxide precipitation, Eq. A-4 and A-6 are inapplicable. Instead, inequalities A-1-1 and A-1-3 apply. Also,

$$X1 = X3 = 0 \quad (A-3-1)$$

and substituting these values in Eq. A-1, 2 and 3:

$$C + X2 = C0 \quad (A-3-2)$$

$$S1 + S2 = S0 \quad (A-3-3)$$

$$M = M0 \quad (A-3-4)$$

Eq. A-5 is valid in the present case. Eq. A-8 and the electroneutrality equation A-10, remain valid.

Eliminating  $S2$  between Eq. A-8 and A-3-3:

$$S1 = K5 * S0 / (K5 + \emptyset) \quad (A-3-5)$$

Substitution in the electroneutrality equation A-10 for  $M$ ,  $(S1 + S2)$  and  $S1$  from Eq. A-3-4, A-3-3 and A-3-5, respectively, yields:

$$A + 2 * C + 2 * (M0 - S0) + K1/\emptyset - \emptyset + K5 * S0 / (K5 + \emptyset) = 0 \quad (A-3-6)$$

Simultaneous solution of Eq. A-5 and A-3-6 yields values for  $C$  and/or  $\emptyset$ . The pH is then expressed by Eq. A-1-12.

#### CASE (4), MAGNESIUM HYDROXIDE PRECIPITATION

This case is symmetrical with case (1). The same equations are obtained with exchange of  $X_3$ ,  $M$ ,  $M_0$  and  $K_3$  with  $X_2$ ,  $C$ ,  $C_0$  and  $K_4$ , respectively:

$$X_1 = X_2 = 0 \quad (A-4-1)$$

$$M + X_3 = M_0 \quad (A-4-2)$$

$$S_1 + S_2 = S_0 \quad (A-4-3)$$

$$C = C_0 \quad (A-4-4)$$

$$S_1 = K_5 * \emptyset / (K_5 + \emptyset) \quad (A-4-5)$$

$$A + 2 * M + 2 * (C_0 - S_0) + K_1/\emptyset - \emptyset + K_5 * S_0 / (K_5 + \emptyset) = 0 \quad (A-4-6)$$

Eq. A-1 and A-5 are inapplicable. Instead, inequalities A-1-1 and A-1-2 apply. Eq. A-6 is valid.

Simultaneous solution of Eq. A-6 and A-4-6 yields values for  $M$  and/or  $\emptyset$ . The pH is then expressed by Eq. A-1-12.

#### CASE (5), CALCIUM SULFATE AND CALCIUM HYDROXIDE PRECIPITATION

In this case, Eq. A-6 is inapplicable. Instead, inequality A-1-3 applies. Also,

$$X_3 = 0 \quad (A-5-1)$$

and substituting this value in Eq. A-3:

$$M = M_0 \quad (A-5-2)$$

Eq. A-1, A-2, A-4 and A-5 are valid in the present case. Eq. A-8 and the electroneutrality equation A-10 remain valid.

From Eq. A-4 and A-8, respectively:

$$S_2 = K_6/C \quad (A-5-3)$$

and

$$S_1 = (K_5/\emptyset) (K_6/C) \quad (A-5-4)$$

Substitution into the electroneutrality equation A-10, for  $M$ ,  $S_2$  and  $S_1$  from Eq. A-5-2, A-5-3, and A-5-4, respectively, yields:

$$A + (2 * C) + (2 * M_0) + K_1/\emptyset - \emptyset - (2 + K_5/\emptyset) (K_6/C) = 0 \quad (A-5-5)$$

Simultaneous solution of Eq. A-5 and A-5-5 yields values for  $C$  and/or  $\emptyset$ . The pH is expressed by Eq. A-1-12.

## CASE (6), CALCIUM SULFATE AND MAGNESIUM HYDROXIDE PRECIPITATION

In this case, Eq. A-5 is inapplicable. Instead, inequality A-1-2 applies. Also,

$$X_2 = 0 \quad (A-6-1)$$

and substituting this value in Eq. A-1:

$$C + X_1 = C_0 \quad (A-6-2)$$

Eq. A-2, A-3, A-4 and A-6 are valid in the present case. Eq. A-6 and the electroneutrality equation A-10 are valid.

Eliminating  $X_1$  between Eq. A-2 and A-6-2, yields:

$$S_1 + S_2 = S_0 - C_0 + C \quad (A-6-3)$$

From Eq. A-4 and A-8, respectively:

$$S_2 = K_6/C \quad (A-6-4)$$

and

$$S_1 = (K_5/\emptyset) (K_6/C) \quad (A-6-5)$$

Substitution of these expressions into Eq. A-6-3 yields:

$$C^2 + (S_0 - C_0) * C - (1 + K_5/\emptyset) K_6 = 0 \quad (A-6-6)$$

A second relation between the two unknowns  $C$  and  $\emptyset$  is obtained by substitution into the electroneutrality equation A-10 for  $M$ ,  $(S_1 + S_2)$  and  $S_1$  from Eq. A-6, A-6-3, and A-6-5, respectively:

$$A + 2 * K_3/\emptyset^2 + K_1/\emptyset - \emptyset - 2 * (S_0 - C_0) + (K_5/\emptyset)(K_6/C) \quad (A-6-7)$$

Simultaneous solution of Eq. A-6-6 and A-6-7 yields the values for  $C$  and/or  $\emptyset$ . The pH is given by Eq. A-1-12.

## CASE (7), CALCIUM AND MAGNESIUM HYDROXIDE PRECIPITATION

In this case, Eq. A-4 is inapplicable. Instead, inequality A-1-1 applies. Also,

$$X_1 = 0 \quad (A-7-1)$$

and substituting this value in Eq. A-1 and A-2:

$$C + X_2 = C_0 \quad (A-7-2)$$

$$S_1 + S_2 = S_0 \quad (A-7-3)$$

Eq. A-3, A-5 and A-6 are valid in the present case. Eq. A-8 and the electro-neutrality equation A-10 remain valid.

Eliminating  $\emptyset$  between Eq. A-5 and A-6 yields:

$$M = K_3 * C/K_4 \quad (A-7-4)$$

Eliminating  $S_2$  between Eq. A-8 and A-7-3 yields:

$$S_1 = K_5 * S_0 / (K_5 + \emptyset) \quad (A-7-5)$$

From Eq. A-5:

$$\emptyset = \sqrt{K_4}/\sqrt{C} \quad (A-7-6)$$

and substitution into Eq. A-7-5:

$$S_1 = K_5 * S_0 * \sqrt{C} / (K_4 + K_5 * \sqrt{C}) \quad (A-7-7)$$

Substitution into the electroneutrality equation A-10, for  $(S_1 + S_2)$ ,  $M$ ,  $\emptyset$ , and  $S_1$  from Eq. A-7-3, A-7-4, A-7-6 and A-7-7, respectively, yields:

$$2 (1 + K_3/K_4) Y^2 + (K_1/\sqrt{K_4}) Y + A - 2 * S_0 + K_5 * S_0 * Y / (\sqrt{K_4} + K_5 * Y) - \sqrt{K_4}/Y = 0 \quad (A-7-8)$$

where  $Y$  is defined as:

$$Y = \sqrt{C} \quad (A-7-9)$$

Solution of Eq. A-7-8 and substitution into A-7-9 and then into A-7-6 yields the value of  $\emptyset$ . The pH is given by Eq. A-1-12.

CASE (8), CALCIUM SULFATE, CALCIUM HYDROXIDE AND MAGNESIUM HYDROXIDE PRECIPITATION  
In this case, all the general equations in the first section are valid.

Elimination of  $\emptyset$  between equations A-5 and A-6 yields:

$$M = K_3 * C/K_4 \quad (A-8-1)$$

From Eq. A-4:

$$S_2 = K_6/C \quad (A-8-2)$$

From Eq. A-5:

$$\emptyset = \sqrt{K_4}/\sqrt{C} \quad (A-8-3)$$

From Eq. A-8:

$$S_1 = K_5 * S_2/\emptyset \quad (A-8-4)$$

Substitution for  $S_2$  from Eq. A-8-2 and for  $\emptyset$  from Eq. A-8-3 yields:

$$S_1 = (K_5/\sqrt{K_4}) (K_6/\sqrt{C}) \quad (A-8-5)$$

Substitution into the electroneutrality equation (A-10) for  $M$ ,  $S_2$ ,  $\emptyset$  and  $S_1$  from Eq. A-8-1, A-8-2, A-8-3 and A-8-5, respectively, yields:

$$2 (1 + K_3/K_4) Y^2 + (K_1/\sqrt{K_4}) Y + A - \\ (\sqrt{K_4} + K_5 * K_6/\sqrt{K_4})/Y - K_6/Y^2 = 0 \quad (A-8-6)$$

where  $Y$  is defined by Eq. A-7-9.

Solution of Eq. A-8-6 and substitution into Eq. A-7-9 and then into Eq. A-8-3 yield the value for  $\emptyset$ . The pH is expressed by Eq. A-1-12.

#### DETERMINATION OF THE RELEVANT SET OF EQUATIONS

Calcium sulfate will not precipitate as long as the ionic product  $C_0 * S_2$  is smaller than the solubility product  $K_6$ , i.e.:

$$C_0 * S_2 < K_6 \quad (A-9-1)$$

Similarly for calcium and magnesium hydroxides:

$$C_0 * \emptyset^2 < K_4 \quad (A-9-2)$$

$$M_0 * \emptyset^2 < K_3 \quad (A-9-3)$$

If  $\emptyset$  and  $S_2$  were known, A-9-1, A-9-2 and A-9-3 would make suitable criteria.

Inequality A-9-1 can be cast in a more suitable form by recalling that Eq. A-8 is valid for all cases and therefore can be applied to express  $S_1$  as:

$$S_1 = (K_5/\emptyset) S_2$$

and adding  $S_2$  on both sides:

$$S_1 + S_2 = (1 + K_5/\theta) S_2$$

from which

$$S_2 = (S_1 + S_2)/(1 + K_5/\theta) \quad (A-9-4)$$

Substitution of this expression for  $S_2$  into inequality A-9-1 and rearrangement, yield:

$$C_0 * (S_1 + S_2) < K_6 * (1 + K_5/\theta) \quad (A-9-5)$$

Moreover, as long as calcium sulfate is not precipitating, then

$$X_1 = 0 \quad (A-9-6)$$

Eq. A-2 becomes

$$S_1 + S_2 = S_0 \quad (A-9-7)$$

and this expression can be substituted into inequality A-9-5 to yield:

$$C_0 * S_0 < K_6 * (1 + K_5/\theta) \quad (A-9-8)$$

Inequality A-9-3 is a necessary and sufficient condition for non-precipitation of magnesium hydroxide. Inequalities A-9-2 and 8 are independently sufficient but not necessary conditions for non-precipitation of calcium hydroxide and calcium sulfate, respectively. That is if either of A-9-2 or A-9-8 (or both) is satisfied, the test is conclusive; if neither is met, additional testing is required. These additional tests are derived by considering that when the calcium ion is in equilibrium with both its hydroxide and its sulfate, the following relations must apply:

$$C = K_4/\theta^2 \quad (A-9-9)$$

and

$$S_0/(1 + K_5/\theta) > S_2 = K_6/C$$

from which:

$$S_0 * C > K_6 * (1 + K_5/\theta) \quad (A-9-10)$$

and substituting for  $C$  from Eq. A-9-9:

$$S_0 * K_4/\theta^2 > K_6 * (1 + K_5/\theta) \quad (A-9-11)$$

If neither of the three inequalities A-9-2, A-9-8 and A-9-11 is met, calcium hydroxide precipitates, but not calcium sulfate.

If only inequalities A-9-2 and A-9-8 are not met, but A-9-11 is verified, calcium sulfate precipitates and one more test is required for calcium hydroxide. For this purpose, the would be calcium concentration in absence of calcium hydroxide precipitation, is calculated from Eq. A-2-8 or from A-6-6 which is identical to A-2-8, and the ionic product is compared to the solubility product. If

$$C * \varnothing^2 > K_4 \quad (A-9-12)$$

the hydroxide precipitates with the sulfate, if not, calcium hydroxide does not precipitate.

The problem now is to determine initially the correct value of  $\varnothing$ . Various procedures are possible. The procedure used in this work is, in principle, as follows:

1. A tentative value  $\varnothing_1$  is guessed for  $\varnothing$ . For an initial solution (before concentrating)  $\varnothing_1$  corresponds to neutral pH at operating temperature. For a residual solution, the last pH value yields the tentative guess for  $\varnothing_1$ .
2. The criteria are used to determine which species would precipitate, i.e., which one of the eight sets of equations applies.
3. The equations are solved and  $\varnothing$  determined.
4. The value  $\varnothing$  is compared to the value  $\varnothing_1$ . If close enough (within a preselected accuracy limit), the case was solved correctly and the value calculated for  $\varnothing$  is its correct value. If the values  $\varnothing$  and  $\varnothing_1$  are not close enough, the previous guess  $\varnothing_1$  is discarded and the value of  $\varnothing$  is assigned to  $\varnothing_1$  as a better guess to repeat the procedure from step 2 and so on until  $\varnothing \sim \varnothing_1$

This procedure allows updating the values of the ionic strength and of the solubility products and other equilibrium constants, at each computational cycle, when the necessary data are available.

In general, the procedure converges because the validity of each of the eight sets of equations covers a wide range of  $\varnothing$  values.

In the case of competing precipitations, it could be suggested that the compound with the highest ratio of ionic to solubility products will precipitate. Consideration is given to this possible criterion in Appendix D.

### VOLATILES

The ions produced by the reversible dissociation of volatile species are removed from the solution in the early stages of the concentrating process, before conditions for participating in the formation of precipitates can be reached. However, during these early stages, these ionic species affect the pH of the solution.

The volatile species considered in this work are carbon dioxide and ammonia, or morpholine or cyclohexylamine. Only ammonia is discussed below.

Ammonia reacts with water to form ammonium hydroxide in equilibrium with the ions formed by dissociation:



Letting  $B$  and  $B1$  represent the concentrations of  $\text{NH}_4\text{OH}$  and  $\text{NH}_4^+$ , respectively, in solution, the equilibrium constant for the reaction A-10-1 is defined as

$$(B1/B) * \phi = K2 \quad (\text{A-10-2})$$

Define also:

$$B/(B + B1) = F2 \quad (\text{A-10-3})$$

From Eq. A-10-2:

$$B1/B = K2/\phi$$

and

$$(B + B1)/B = 1 + B1/B = 1 + K2/\phi = (\phi + K2)/\phi$$

from which

$$F2 = B/(B + B1) = \phi/(\phi + K2) \quad (\text{A-10-4})$$

The distribution coefficient for ammonia is defined as:

$$D2 = \frac{\text{molal concentration of NH}_3 \text{ in vapor phase}}{\text{molal concentration of NH}_4\text{OH in liquid phase}} \quad (\text{A-10-5})$$

Whether ammonia in the vapor mixture is hydrated or not is irrelevant here. To pursue the treatment, the model selected must now be specified.

#### Dynamic Equilibrium Model

Consider an initial liquid mass  $L^\circ$  with total ammonia concentration  $B_0$ , i.e.,

$$B_0 = B^\circ + B_1^\circ \quad (A-10-6)$$

where  $B^\circ$  and  $B_1^\circ$  are the initial concentrations of  $\text{NH}_4\text{OH}$  and  $\text{NH}_4^+$ , respectively, in the initial liquid mass  $L^\circ$ . Let  $L$  and  $V$  represent the masses in the liquid and vapor phases.

A mass balance over the system yields:

$$L + V = L^\circ \quad (A-10-7)$$

Conservation of the ammonia species yields:

$$(B_1 + B)L + D_2 * B * V = B_0 * L^\circ$$

Substitution for  $B$  and for  $V$  from Eq. A-10-3 and A-10-7, respectively, yields:

$$(B_1 + B) * [L + D_2 * F_2 * (L^\circ - L)] = B_0 * L^\circ$$

from which:

$$B_1 + B = B_0 * L^\circ / (L + D_2 * F_2 * (L^\circ - L))$$

or

$$B_1 + B = B_0 / (L/L^\circ + (1 - L/L^\circ) * D_2 * F_2) \quad (A-10-8)$$

Defining a concentration factor as:

$$T_1 = L^\circ/L \quad (A-10-9)$$

and substituting into Eq. A-10-8 yields:

$$B_1 + B = B_0 / (1/T_1 + (1 - 1/T_1) * D_2 * F_2) \quad (A-10-10)$$

From Eq. A-10-3:

$$B = F_2 * (B + B_1)$$

so that

$$B_1 = (B + B_1) - B = (1 - F_2) (B + B_1) \quad (A-10-11)$$

and substituting for  $(B + B1)$  from Eq. A-10-10:

$$B1 = (1 - F2) B0 / (1/T1 + (1 - 1/T1) * D2 * F2) \quad (A.10.12)$$

Similarly for carbon dioxide:

$$H1 = (1 - F7) H0 / (1/T1 + (1 - 1/T1) * D7 * F7) \quad (A.10.13)$$

where  $H1$  represent the concentration of bicarbonate ion  $HCO_3^-$  in the liquid phase,  $H0$  the conserved total amount of  $CO_2$  in its various forms in the two phases,  $D7$  is the partition coefficient for  $CO_2$ :

$$D7 \equiv \frac{\text{molal concentration of } CO_2 \text{ in the vapor phase}}{\text{molal concentration of } H_2CO_3 \text{ in the liquid phase}} \quad (A.10.14)$$

and

$$F7 \equiv (H_2CO_3) / ((H_2CO_3) + (HCO_3^-)) = K7 / (K7 + \emptyset) \quad (A.10.15)$$

where  $K7$  is the equilibrium constant

$$K7 = (H_2CO_3) \emptyset / (HCO_3^-) \quad (A.10.16)$$

for the equilibrium:



The second dissociation equilibrium



is neglected because practically all the carbon dioxide escapes very early in the concentrating process before the pH can change sufficiently to make the concentration of  $CO_3^{\equiv}$  appreciable.

Eq. A-10-12 and A-10-13 determine the ionic contributions of ammonia and of carbon dioxide, respectively, in the liquid residue as the steam quality of the constant mass is increased at constant temperature and pressure.

#### Isolated Cavity Model

Consider a differential mass  $dL$  escaping from a residual liquid mass  $L$  with molal concentrations  $B1$  and  $B$  of  $NH_4^+$  and  $NH_4OH$ , respectively.

The concentration of ammonia in  $dL$  is  $(D2 * B)$  and the number of moles of ammonia escaping in  $dL$  is then:

$$d[(B + B1) * L] = D2 * B * dL \quad (A-10-19)$$

but

$$d[(B + B1) * L] = (B + B1) * dL + L * d(B + B1) \quad (A-10-20)$$

Comparison with Eq. A-10-19 yields:

$$[(D2 * B) - (B + B1)]dL = L * d(B + B1)$$

and substituting for B in the first term on the left side, from Eq. A-10-3:

$$(D2 * F2 - 1) (B + B1) * dL = L * d(B + B1)$$

or

$$d(B + B1)/(B + B1) = (D2 * F2 - 1) * dL/L \quad (A-10-21)$$

From Eq. A-10-4 it is seen that F2 is a function of pH and of K2, and both these are functions of the total composition. Nevertheless, Eq. A-10-21 may be solved by integrating on both sides over a small range for which F2 does not vary appreciably, yielding:

$$\log ((B + B1)_{n+1}/(B + B1)_n) = (D2 * F2 - 1) * \log (L_{n+1}/L_n)$$

or

$$(B + B1)_{n+1} = (B + B1)_n (T1_n/T1_{n+1})^{(D2 * F2 - 1)}$$

and since F2 has not varied appreciably over the small range from T1<sub>n</sub> to T1<sub>n+1</sub>,

$$B1_{n+1} = B1_n (T1_n/T1_{n+1})^{(D2 * F2 - 1)} \quad (A-10-22)$$

Alternatively, for such a small step, Eq. A-10-21 can be cast in the form of a difference equation:

$$((B + B1)_{n+1} - (B + B1)_n)/(B + B1)_n = (D2 * F2 - 1) (L_{n+1} - L_n)/L_n$$

or

$$(B + B1)_{n+1}/(B + B1)_n = 1 + D2 * F2 - 1 * (T1_n/T1_{n+1} - 1)$$

and since the ratio F2 (Eq. A-10-4) has not changed appreciably:

$$(B1)_{n+1} = (B1)_n * (1 - (D2 * F2 - 1) * (1 - T1_n/T1_{n+1})) \quad (A-10-23)$$

Eq. A-10-21 can be solved over a wide range by using either of Eq. A-10-22 or A-10-23 over successive small steps and updating the value of F2 by determining the chemistry of the residual solution after each small incremental step.

Similarly for carbon dioxide with the following two equations:

$$H_{n+1} = H_n (T_n/T_{n+1})^{(D7 * F7 - 1)} \quad (A.10.24)$$

$$H_{n+1} = H_n * (1 - (D7 * F7 - 1)) * (1 - T_n/T_{n+1}) \quad (A.10.25)$$

corresponding to Eq. A-10-22 and A-10-23, respectively.

## LIST OF SYMBOLS

A	An algebraic sum defined by Eq. A-11.
B	Concentration of neutral species $\text{NH}_4\text{OH}$ in the liquid, mole/kg.
B1	Concentration of cation $\text{NH}_4^+$ in the liquid, mole/kg.
$B^\circ$ , $B1^\circ$	Initial values (before concentrating) of B and B1, respectively. mole/kg.
$B0$	$(\equiv B^\circ + B1^\circ)$ , mole/kg.
C	Concentration of calcium ion $\text{Ca}^{++}$ in the liquid, mole/kg.
$C0$	Total calcium in residue (liquid + precipitate), mole/kg.
D2	Vapor/liquid partition coefficient for ammonia.
D7	Vapor/liquid partition coefficient for carbon dioxide.
F2	Fraction of undissociated ammonia in the liquid $[\equiv \text{NH}_4\text{OH}/(\text{NH}_4\text{OH} + \text{NH}_4^+)]$ .
F7	Fraction of undissociated carbonic acid in the liquid $[\equiv \text{H}_2\text{CO}_3/(\text{H}_2\text{CO}_3 + \text{HCO}_3^-)]$ .
H1	Concentration of bicarbonate anion $\text{HCO}_3^-$ in the liquid, mole/kg.
$H0$	Initial concentration (before evaporating) of total carbon dioxide $(\text{H}_2\text{CO}_3 + \text{HCO}_3^-)$ in the liquid, mole/kg.
I	Ionic strength, $(\text{mole equivalent})^2/\text{mole/kg}$ .
$I1$	Tentative value of ionic strength, $(\text{mole equivalent})^2/\text{mole/kg}$ .
K1	Ionic product for water, $(\text{mole/kg})^2$ .
K2	Equilibrium constant for ammonia dissociation in aqueous solutions, mole/kg.
K3	Solubility product for magnesium hydroxide, $(\text{mole/kg})^3$ .
K4	Solubility product for calcium hydroxide, $(\text{mole/kg})^3$ .
K5	Sulfate/bisulfate equilibrium constant defined by Eq. A-8, mole/kg.
K6	Solubility product for calcium sulfate, $(\text{mole/kg})^2$ .
K7	Equilibrium constant for first dissociation of carbonic acid in aqueous solutions, mole/kg.
L	Mass of the liquid, kg.
$L^\circ$	Initial mass of the liquid, kg.
$L1$	Concentration of chloride ion $\text{Cl}^-$ in the liquid, mole/kg.
M	Concentration of magnesium ion $\text{Mg}^{++}$ in the liquid, mole/kg.
$M0$	Total magnesium in residue (liquid + precipitate), mole/kg.

N Concentration of sodium ion  $\text{Na}^+$  in the liquid, mole/kg.  
Ø Concentration of hydroxyl ion  $\text{OH}^-$  in the liquid, mole/kg.  
P1 pH of liquid.  
S1 Concentration of bisulfate ion  $\text{HSO}_4^-$  in the liquid, mole/kg.  
S2 Concentration of sulfate ion  $\text{SO}_4^{=}$  in the liquid, mole/kg.  
S0 Total sulfur (bisulfate + sulfate in liquid and in precipitate) in residue, mole/kg.  
T1 Concentration factor ( $\equiv L^\circ / L$ ).  
V Mass of vapor, kg.  
X1 Precipitated calcium sulfate in residue, mole/kg.  
X2 Precipitated calcium hydroxide in residue, mole/kg.  
X3 Precipitated magnesium hydroxide in residue, mole/kg.

## Appendix B

### DERIVATION OF THE SOLUBILITY PRODUCT FOR SERPENTINE FROM THERMODYNAMIC DATA

The precipitation of magnesium hydroxide can be expressed as:



from which the solubility product  $K_3$  is defined as:

$$K_3 = [\text{Mg}^{++}] * [\text{OH}^-]^2$$

Neglecting ionic strength,  $K_3$  can be represented by:

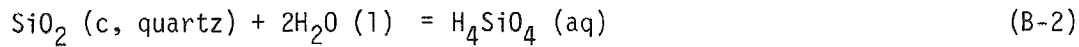
$$\text{Log } K_3 = 31.31 + 12.9722 \text{ Log } T - 530.49/T - 0.032331 T$$

which at  $T = 275^\circ\text{C} = 548^\circ\text{K}$ , yields  $\text{Log } K_3 = -14.47$  from which the free energy,  $\Delta G_1$  for the precipitation reaction is:

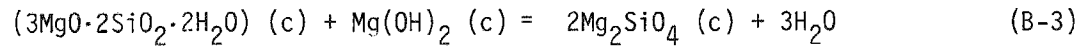
$$\Delta G_1 = -2.3026 RT (-\text{Log } K_3) = -36,300 \text{ calories/mole}$$

where  $R$  is the ideal gas constant (1.986 calories/mole/°K).

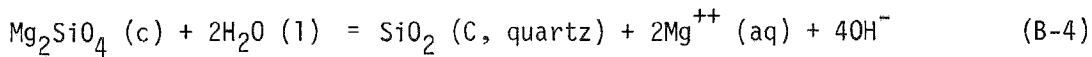
From Reference 11, the following reactions and their corresponding free energies (at 275°C) are obtained:



$$\Delta G_2 = +5180 \text{ calories/mole}$$

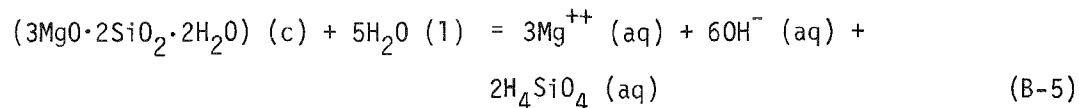


$$\Delta G_3 = +2,700 \text{ calories/mole}$$



$$\Delta G_4 = +77,000 \text{ calories/mole}$$

Linear combination of the four reactions B-1 through B-4 yields the solubilization reaction for serpentine:



$$\Delta G_5 = 130,760 \text{ calories/mole}$$

from which the solubility product  $H_4$  is defined as:

$$H_4 \equiv [Mg^{++}]^3 * [OH^-]^6 * [H_4SiO_4]^2 \quad (B-6)$$

$$\log H = -\Delta G_5 / 2.3026 RT = -52.18 \quad (B-7)$$

## Appendix C

### PHASE DIAGRAM CONSTRUCTION

The logarithms of solubility products at 275°C for the fourteen compounds initially considered are given in Table C-1.

To determine the stability of these compounds in water, their possible reaction with water are considered, and the free energy of these reactions calculated from the data in reference 11. Five of the compounds were found to have no region of stability on the phase diagram to be constructed and as such did not warrant further consideration. These compounds, their reactions and corresponding free energies are given in Table C-2.

As shown in Figure C-1, the plane of the phase diagram is defined by  $\log (\text{Mg}^{++}/\text{Ca}^{++})$  along the abscissa and by  $\log (\text{H}_4\text{SiO}_4, \text{aqueous})$  along the ordinate. Three groups of boundaries can be distinguished:

1. Boundaries independent of the  $(\text{Mg}^{++}/\text{Ca}^{++})$  ratio will be horizontal lines at a fixed value of  $(\text{H}_4\text{SiO}_4, \text{aqueous})$ .
2. Boundaries independent of the  $(\text{H}_4\text{SiO}_4, \text{aqueous})$  value will be vertical lines at a fixed  $(\text{Mg}^{++}/\text{Ca}^{++})$  ratio.
3. The other boundaries are straight lines with finite slopes.

Examples for the determination of a boundary in each of these groups follow:

1. Consider  $\text{CaSiO}_3$  and  $\text{Ca}_3\text{Si}_2\text{O}_7$ . At the boundary between their domains of relative stability, they both exist, i.e., both solubility products are valid and from Table C-1:

$$\log [\text{Ca}^{++}] [\text{OH}^-]^2 [\text{H}_4\text{SiO}_4^\circ] = -15.70 \quad (\text{C-1})$$

$$\log [\text{Ca}^{++}]^3 [\text{OH}^-]^6 [\text{H}_4\text{SiO}_4] = -43.16 \quad (\text{C-2})$$

Multiplying Eq. C-1 on both sides by 3, yields:

$$\log [\text{Ca}^{++}]^3 [\text{OH}^-]^6 [\text{H}_4\text{SiO}_4^\circ]^3 = -47.10 \quad (\text{C-3})$$

Table C-1  
SOLUBILITY RELATIONS

Solubilization Reaction
$\text{SiO}_2 + 2\text{H}_2\text{O} = \text{H}_4\text{SiO}_4^\circ$
$\text{CaSiO}_3 + 3\text{H}_2\text{O} = \text{Ca}^{++} + 2\text{OH}^- + \text{H}_4\text{SiO}_4^\circ$
$\text{Ca}_3\text{Si}_2\text{O}_7 + 7\text{H}_2\text{O} = 3\text{Ca}^{++} + 6\text{OH}^- + 2\text{H}_4\text{SiO}_4^\circ$
$\text{Ca}_2\text{SiO}_4 + 4\text{H}_2\text{O} = 2\text{Ca}^{++} + 4\text{OH}^- + \text{H}_4\text{SiO}_4^\circ$
$\text{Ca}_3\text{SiO}_5 + 5\text{H}_2\text{O} = 3\text{Ca}^{++} + 6\text{OH}^- + \text{H}_4\text{SiO}_4^\circ$
$\text{Ca}(\text{OH})_2 = \text{Ca}^{++} + 2\text{OH}^-$
$\text{CaMgSi}_2\text{O}_6 + 6\text{H}_2\text{O} = \text{Ca}^{++} + \text{Mg}^{++} + 4\text{OH}^- + 2\text{H}_4\text{SiO}_4^\circ$
$\text{Ca}_2\text{MgSi}_2\text{O}_7 + 7\text{H}_2\text{O} = 2\text{Ca}^{++} + \text{Mg}^{++} + 6\text{OH}^- + 2\text{H}_4\text{SiO}_4^\circ$
$\text{CaMgSiO}_4 + 4\text{H}_2\text{O} = \text{Ca}^{++} + \text{Mg}^{++} + 4\text{OH}^- + \text{H}_4\text{SiO}_4^\circ$
$\text{MgSiO}_3 + 3\text{H}_2\text{O} = \text{Mg}^{++} + 2\text{OH}^- + \text{H}_4\text{SiO}_4^\circ$
$\text{Mg}_3\text{Si}_2\text{O}_7 \cdot 2\text{H}_2\text{O} + 5\text{H}_2\text{O} = 3\text{Mg}^{++} + 6\text{OH}^- + 2\text{H}_4\text{SiO}_4^\circ$
$\text{Mg}_2\text{SiO}_4 + 4\text{H}_2\text{O} = 2\text{Mg}^{++} + 4\text{OH}^- + \text{H}_4\text{SiO}_4^\circ$
$\text{Mg}(\text{OH})_2 = \text{Mg}^{++} + 2\text{OH}^-$
$\text{CaSO}_4 = \text{Ca}^{++} + \text{SO}_4^=$

Log of Solubility Products at 275°C
$\text{Log } [\text{H}_4\text{SiO}_4^\circ] = - 2.06$
$\text{Log } [\text{Ca}^{++}] [\text{OH}^-]^2 [\text{H}_4\text{SiO}_4^\circ] = - 15.70$
$\text{Log } [\text{Ca}^{++}]^3 [\text{OH}^-]^6 [\text{H}_4\text{SiO}_4^\circ]^2 = - 43.16$
$\text{Log } [\text{Ca}^{++}]^2 [\text{OH}^-]^4 [\text{H}_4\text{SiO}_4^\circ] = - 25.33$
$\text{Log } [\text{Ca}^{++}]^3 [\text{OH}^-]^6 [\text{H}_4\text{SiO}_4^\circ] = - 29.6$
$\text{Log } [\text{Ca}^{++}] [\text{OH}^-]^2 = - 8.88$
$\text{Log } [\text{Ca}^{++}] [\text{Mg}^{++}] [\text{OH}^-]^4 [\text{H}_4\text{SiO}_4^\circ]^2 = - 35.47$
$\text{Log } [\text{Ca}^{++}]^2 [\text{Mg}^{++}] [\text{OH}^-]^6 [\text{H}_4\text{SiO}_4^\circ]^2 = - 45.46$
$\text{Log } [\text{Ca}^{++}] [\text{Mg}^{++}] [\text{OH}^-]^4 [\text{H}_4\text{SiO}_4^\circ] = - 30.68$
$\text{Log } [\text{Mg}^{++}] [\text{OH}^-]^2 [\text{H}_4\text{SiO}_4^\circ] = - 18$
$\text{Log } [\text{Mg}^{++}]^3 [\text{OH}^-]^6 [\text{H}_4\text{SiO}_4^\circ]^2 = - 52.14$
$\text{Log } [\text{Mg}^{++}]^2 [\text{OH}^-]^4 [\text{H}_4\text{SiO}_4^\circ] = - 32.77$
$\text{Log } [\text{Mg}^{++}] [\text{OH}^-]^2 = - 14.48$
$\text{Log } [\text{Ca}^{++}] [\text{SO}_4^=] = - 9.03$

Table C-2  
 FREE ENERGY OF REACTIONS  
 275°C

<u>Reaction</u>	<u>Free Energy at 275°C</u>
$2\text{Ca}_2\text{SiO}_4 + \text{H}_2\text{O} \rightarrow \text{Ca}_3\text{Si}_2\text{O}_7 + \text{Ca}(\text{OH})_2$	- 3,460
$2\text{Ca}_3\text{SiO}_5 + 3\text{H}_2\text{O} \rightarrow \text{Ca}_3\text{Si}_2\text{O}_7 + 3\text{Ca}(\text{OH})_2$	- 26,600
$\text{Ca}_2\text{MgSi}_2\text{O}_7 + \text{H}_2\text{O} \rightarrow 2\text{CaSiO}_3 + \text{Mg}(\text{OH})_2$	- 26,130
$3\text{MgSiO}_3 + 2\text{H}_2\text{O} \rightarrow \text{SiO}_2 + \text{Mg}_3\text{Si}_2\text{O}_7 \cdot 2\text{H}_2\text{O}$	- 500
$2\text{Mg}_2\text{SiO}_4 + 3\text{H}_2\text{O} \rightarrow \text{Mg}_3\text{Si}_2\text{O}_7 \cdot 2\text{H}_2\text{O} + \text{Mg}(\text{OH})_2$	- 84,900

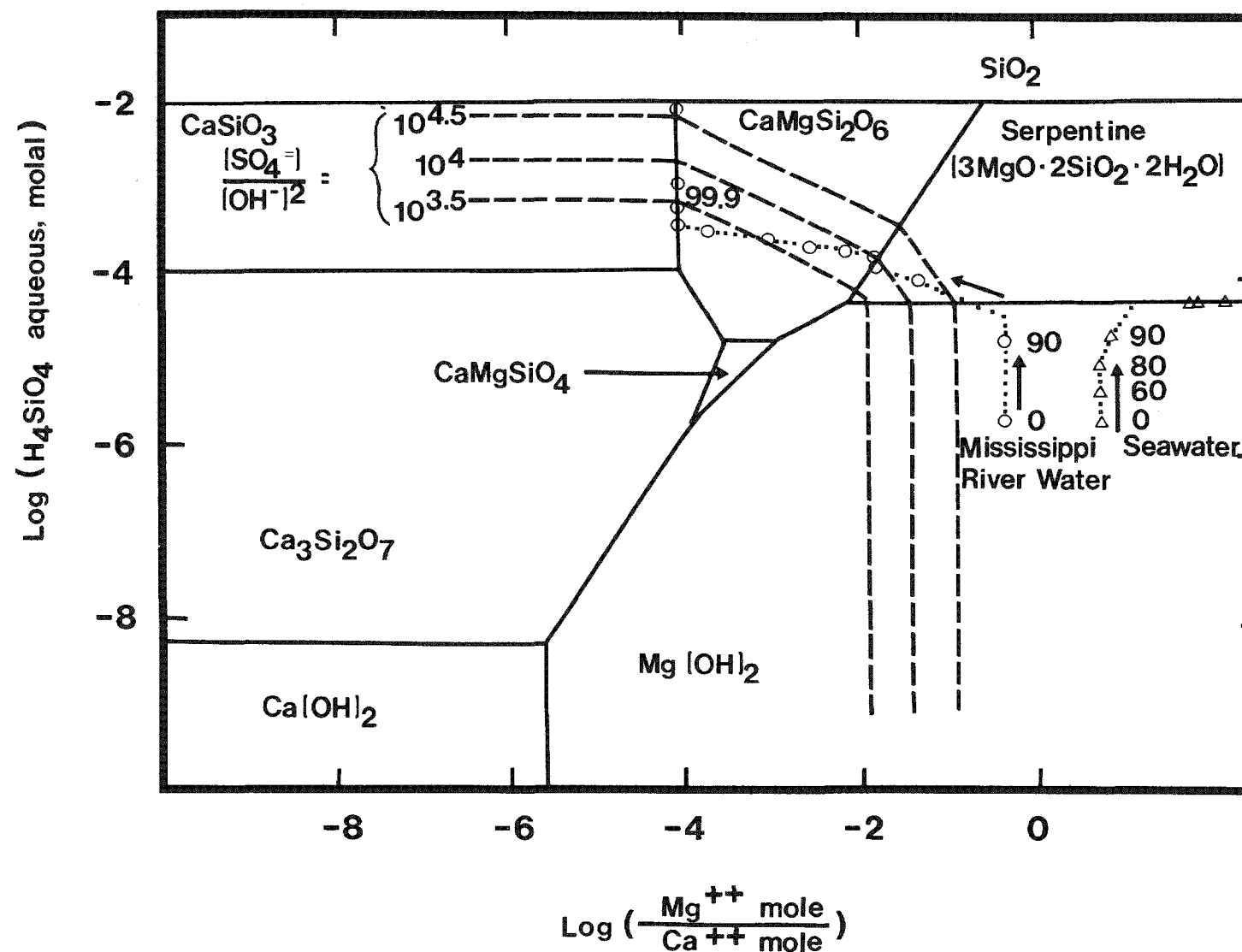


Figure C-1. Phase Diagram of Relative Stabilities at 275°C

Subtracting C-2 from C-3 yields:

$$\log [H_4SiO_4^\circ] = -3.94 \quad (C-4)$$

Eq. C-4 represents the horizontal straight line boundary between the domains of relative stabilities of  $CaSiO_3$  and  $Ca_3Si_2O_7$  on the phase diagram of Figure C-1.

2. Similarly, for  $CaSiO_3$  and  $CaMgSi_2O_6$  from Table C-1:

$$\log [Ca^{++}] [OH^-]^2 [H_4SiO_4^\circ]^2 = -15.70 \quad (C-5)$$

$$\log [Ca^{++}] [Mg^{++}] [OH^-]^4 [H_4SiO_4^\circ]^2 = -35.47 \quad (C-6)$$

Eq. C-5 can be written:

$$\log [Ca^{++}]^2 [OH^-]^4 [H_4SiO_4^\circ]^2 = -31.40 \quad (C-7)$$

and subtraction from Eq. C-6 yields:

$$\log ([Mg^{++}]/[Ca^{++}]) = -4.07 \quad (C-8)$$

Eq. C-8 represents the vertical straight line boundary between the domains of relative stabilities of  $CaSiO_3$  and  $CaMgSi_2O_6$ .

3. For  $CaMgSi_2O_6$  and  $Mg_3Si_2O_7 \cdot 2H_2O$  (serpentine) from Table C-1:

$$\log [Ca^{++}] [Mg^{++}] [OH^-]^4 [H_4SiO_4^\circ]^2 = -35.47 \quad (C-9)$$

$$\log [Mg^{++}]^3 [OH^-]^6 [H_4SiO_4^\circ]^2 = -52.14 \quad (C-10)$$

Multiplying by 2/3 on both sides of Eq. C-10:

$$\log [Mg^{++}]^2 [OH^-]^4 [H_4SiO_4^\circ]^{4/3} = -34.76 \quad (C-11)$$

Subtracting C-9 from C-11 and rearranging yields:

$$\log [H_4SiO_4^\circ] = -1.06 + 3/2 \log ([Mg^{++}]/[Ca^{++}]) \quad (C-12)$$

Eq. C-12 represents the straight line boundary between the domains of relative stabilities of  $CaMgSi_2O_6$  and serpentine (slope +1.5 and intercept -1.06).

The boundaries between domains of stability of calcium- and/or magnesium-containing silicates are fixed on the defined plane. However, relative to calcium sulfate, the boundaries depend also on the  $[SO_4^{=2-}]/[OH^-]^2$  ratio and will be

represented by a family of lines, again grouped as horizontal, vertical and other straight lines depending upon the stable silica compound competing with the sulfate.

1. Consider  $\text{CaSiO}_3$  and  $\text{CaSO}_4$ . From Table C-1:

$$\log [\text{Ca}^{++}] [\text{OH}^-]^2 [\text{H}_4\text{SiO}_4^\circ] = -15.70 \quad (\text{C-13})$$

$$\log [\text{Ca}^{++}] [\text{SO}_4^=] = -9.03 \quad (\text{C-14})$$

Subtracting C-13 from C-14 and rearranging:

$$\log [\text{H}_4\text{SiO}_4^\circ] = \log ([\text{SO}_4^=]/[\text{OH}^-]^2) - 6.67 \quad (\text{C-15})$$

For any value of  $[\text{SO}_4^=]/[\text{OH}^-]^2$  Eq. C-15 represents a horizontal straight line boundary between the domains of relative stabilities of  $\text{CaSiO}_3$  and  $\text{CaSO}_4$ , on Figure C-1.

2. Similarly, for magnesium hydroxide and calcium sulfate, from Table C-1:

$$\log [\text{Mg}^{++}] [\text{OH}^-]^2 = -14.48 \quad (\text{C-16})$$

$$\log [\text{Ca}^{++}] [\text{SO}_4^=] = -9.03 \quad (\text{C-17})$$

Subtraction and rearrangement yield:

$$\log ([\text{Mg}^{++}]/[\text{Ca}^{++}]) = \log ([\text{SO}_4^=]/[\text{OH}^-]^2) - 5.45 \quad (\text{C-18})$$

For any value of  $[\text{SO}_4^=]/[\text{OH}^-]^2$ , Eq. C-18 represents a vertical straight line boundary between the domains of relative stabilities of magnesium hydroxide and calcium sulfate.

3. For serpentine and calcium sulfate, from Table C-1:

$$\log [\text{Mg}^{++}]^3 [\text{OH}^-]^6 [\text{H}_4\text{SiO}_4^\circ]^2 = -52.14 \quad (\text{C-19})$$

$$\log [\text{Ca}^{++}] [\text{SO}_4^=] = -9.03 \quad (\text{C-20})$$

Dividing by 3 on both sides of Eq. C-19:

$$\log [\text{Mg}^{++}] [\text{OH}^-]^2 [\text{H}_4\text{SiO}_4^\circ]^{2/3} = -17.38 \quad (\text{C-21})$$

Subtracting side by side from Eq. C-20 and rearranging:

$$\log [\text{H}_4\text{SiO}_4^\circ] = -12.52 - 3/2 \log ([\text{Mg}^{++}]/[\text{Ca}^{++}]) + 3/2 \log ([\text{SO}_4^=]/[\text{OH}^-]^2) \quad (\text{C-22})$$

For any value of  $[\text{SO}_4^{=}] / [\text{OH}^-]^2$ , Eq. C-22 represents a straight line boundary between the domains of relative stabilities of serpentine and calcium sulfate (slope -1.5).

## Appendix D

### PRECIPITATION CRITERION

Consider the case of hydroxyl and sulfate ions competing for calcium to precipitate calcium hydroxide and/or calcium sulfate. The ions in solution are  $H^+$ ,  $OH^-$ ,  $Ca^{++}$ ,  $SO_4^{=}$  and  $HSO_4^-$ . For ease of writing the concentration of these ions, they will be represented by  $H$ ,  $\emptyset$ ,  $C$ ,  $S2$  and  $S1$ , respectively. For simplicity, ionic strength will be neglected.

Two chemical equilibria apply:

$$H \emptyset = K1 \quad (D-1)$$

$$\emptyset S1/S2 = K5 \quad (D-2)$$

Electrical charge balance yields:

$$H + 2C = \emptyset + S1 + 2 S2 \quad (D-3)$$

Let  $Y6$  and  $Y4$  represent the ionic products for calcium sulfate and calcium hydroxide respectively, i.e.,:

$$Y6 = C * S2 \quad \text{and} \quad Y4 = C \emptyset^2 \quad (D-4)$$

It is required to investigate the assumption that if the following inequalities hold initially:

$$Y4_i/K4 > Y6_i/K6 > 1 \quad (D-5)$$

where  $K6$  and  $K4$  are the solubility products for calcium sulfate and calcium hydroxide, respectively, then the latter (i.e., calcium hydroxide) must precipitate. Subscript  $i$  indicates initial values. For this purpose, the hypothesis that the opposite can hold true will be tested, i.e., that in some cases where inequalities (5) are verified, only calcium sulfate will precipitate. In such cases, the material balance on calcium and on sulfate yields:

$$S0 - S1 - S2 = CO - C \quad (D-6)$$

where  $S0$  and  $CO$  are total sulfate and total calcium, respectively.

Substituting for  $H$  from Eq. D-1 and for  $S_1 + S_2$  from Eq. D-6, into Eq. D-3 yields:

$$(K_1/\emptyset) + C = \emptyset + S_2 + S_0 - C_0 \quad (D-7)$$

In logarithmic form Eq. D-2 becomes:

$$\ln \emptyset + \ln S_1 - \ln S_2 = \ln K_5 \quad (D-8)$$

Taking the differential on both sides of Eq. D-6, D-7 and D-8 and rearranging:

$$dS_1 + dS_2 = dC \quad (D-9)$$

$$(1 + K_1/\emptyset^2) d\emptyset + dS_2 = dC \quad (D-10)$$

$$d\emptyset/\emptyset + dS_1/S_1 = dS_2/S_2 \quad (D-11)$$

Solving Eq. D-9, D-10 and D-11 for  $dS_1$ ,  $dS_2$  and  $d\emptyset$ , yields:

$$d\emptyset/dC = 1/((S_2/\emptyset) + (1 + (K_1/\emptyset^2)) (1 + (S_2/S_1))) \quad (D-12)$$

$$dS_1/dC = 1/((\emptyset S_2/(K_1 + \emptyset^2)) + (1 + (S_2/S_1))) \quad (D-13)$$

$$dS_2/dC = ((S_2/S_1) + (\emptyset S_2/(K_1 + \emptyset^2)))/((\emptyset S_2/(K_1 + \emptyset^2)) + (1 + (S_2/S_1))) \quad (D-14)$$

Consider now the ratio

$$Z = (Y_6/K_6)/(Y_4/K_4) = (K_4/K_6) (S_2/\emptyset^2) \quad (D-15)$$

from which the derivation with respect to  $C$  is:

$$dZ/dC = ((1/\emptyset^2) dS_2/dC - 2 (S_2/\emptyset^3) d\emptyset/dC) K_4/K_6 \quad (D-16)$$

Substituting for  $d\emptyset/dC$  and  $dS_2/dC$  from Eq. D-12 and D-14, respectively, and rearranging:

$$dZ/dC = K_4((K_1 + \emptyset^2)/\emptyset/K_5 - S_2/\emptyset)/((1 + K_1/\emptyset^2)(1 + S_2/S_1) + S_2/\emptyset)/K_6/\emptyset^2 \quad (D-17)$$

which can be cast into the following (using Eq. D-1 and D-2);

$$dZ/dC = (K_4/K_6) (H + \emptyset - S_1)/((1 + S_1/S_2) (H + \emptyset) + S_1 S_2)/\emptyset^2 \quad (D-18)$$

Dividing by Eq. D-15 side by side and rearranging:

$$(1/Z) dZ/dC + (H + \emptyset - S_1)/((S_1 + S_2) (H + \emptyset) + S_1 S_2) \quad (D-19)$$

For the practical case of seawater ingress (through condenser inleakage) into steam generators, the residual solution becomes acidic as steam quality increases. Under such conditions,  $\emptyset$  and  $S_2$  are negligible compared to  $H$  and  $S_1$ , respectively. Then, Eq. D-19 is closely approximated by:

$$(1/Z) dZ/dC = (H + \emptyset - S_1)/((H + S_2)S_1) \quad (D-20)$$

The inequality

$$-1/(H + S_2) < (1/Z) dZ/dC < 0 \quad (D-21)$$

will be satisfied provided

$$H + \emptyset < S_1 \quad (D-22)$$

When the difference between  $H$  and  $S_1$  is sufficiently small, precipitation of calcium sulfate from acidic solution will lead to a negligible variation in the relative magnitude of the ratio  $Z$ . However, when  $S_1$  is appreciably larger than  $H$ , the variation can be very large. For example, consider the case:

$$S_1 f = 2 H f \quad (D-23)$$

where subscript  $f$  indicates final values. From Eq. D-20, noting  $S_2 \ll S_1$ :

$$dZ/Z > -dC/2H_f \quad (D-24)$$

and integration on both sides yields:

$$\ln (Z_f/Z_i) > (C_i - C_f)/2 H_f > 0 \quad (D-25)$$

It is then seen that there can be conditions for which:

$$0 < Z_i < 1 < Z_f = K_4/Y_4_f \quad (D-26)$$

where the equality  $Y_6 f = K_6$  was used in the last step. The relations D-26 yield:

$$Y_4 f < K_4 f$$

consistent with the hypothesis that in certain cases calcium hydroxide might not precipitate even though inequalities D-5 apply initially.